(i-STAT system; Abbott Point of Care Inc.), and pH, partial pressures of carbon dioxide ($PaCO_2$) (mm Hg), partial pressures of oxygen (PaO_2) (mm Hg), arterial oxygen saturation (SaO_2) (%), hemoglobin (Hb) (g/dL), and hematocrit (Ht) (%) were measured. The rectal temperature was also monitored and automatically maintained at 37° with a body heating pad system (TR-200; Muromachi Kikai Co., Ltd.).

Experiments in Ischemia Model

In 2 rats, the left middle cerebral artery (MCA) was occluded intraluminally by inserting a nylon 4-0 surgical monofilament with dental impression material into the left common carotid artery (*15*). PET was performed at 30 min after the occlusion without reperfusion.

All animal experiments were performed in compliance with the guidelines of the Laboratory Investigation Committee of Osaka University Graduate School of Medicine.

Quantitative Data Calculation

Regional CBF, regional OEF, and regional $CMRO_2$ were calculated by the steady-state method (*11,12*). Regional CBV was calculated after brief administration by inhalation of ^{15}O-CO gas, which was tightly bound to hemoglobin. In the ^{15}O-CO_2 study, the activity measured in the brain was from ^{15}O-labeled water, which was transferred from $C^{15}O_2$ to $H_2{}^{15}O$ in the pulmonary alveolar capillaries. In the ^{15}O-O_2 study, the activity in the brain was considered to be a sum of 3 components: ^{15}O-labeled water produced as a metabolite of ^{15}O-O_2 in the brain tissues, recirculating ^{15}O-labeled water, and ^{15}O-O_2 fixed to hemoglobin in the vascular compartment. Quantitative values were calculated using the following equations:

$$\text{regional CBF} = \lambda/(C_a/C_t - 1/\rho),$$

$$\text{regional OEF} = \left(C_t'/C_t \times C_a/C_p' - C_a/C_p\right) \Big/ \left(C_a'/C_p' - C_a/C_p\right),$$

$$\text{regional } CMRO_2 = \text{CBF} \times \text{OEF} \times [\text{Total blood oxygen content}],$$

$$\text{regional CBV} = C_t''/(C_a'' \times f),$$

where λ (/min) is the decay constant of ^{15}O. C_a (Bq/g) is the $H_2{}^{15}O$ concentration in the whole blood, C_p (Bq/g) is the $H_2{}^{15}O$ concentration in the blood plasma, and C_t (Bq/mL) is the average brain radioactivity concentration without decay correction in the ^{15}O-CO_2 study. ρ is a brain–blood partition coefficient for water, fixed at 0.91 mL/g (*16*). C_a' (Bq/g) is the $H_2{}^{15}O$ and ^{15}O-O_2 concentration in the whole blood, C_p' (Bq/g) is the $H_2{}^{15}O$ concentration in the blood plasma, and C_t' (Bq/mL) is the average brain radioactivity concentration without decay correction in the ^{15}O-O_2 study. Total blood oxygen content was calculated using the following equation: $1.39 \times$ Hb (g/dL) $\times$ SaO_2 (%)/100 + $0.0031 \times$ PaO_2 (mm Hg). C_a'' (Bq/g) is the ^{15}O-CO concentration in the whole blood, and C_t'' (Bq/mL) is the average brain radioactivity concentration with decay correction in the ^{15}O-CO study. f is the correction value of the hematocrit between the great vessels and the brain, fixed at 0.70 (*17*). The CBV data were used to correct for intravascular hemoglobin-bound $^{15}O_2$ (*12*). Functional images of the CBF, $CMRO_2$, OEF, and CBV were reconstructed using the Shimadzu PET console system. ROIs ($0.86-1.08$ cm^2) were manually drawn on the whole brain of the 3 sequential cross-sectional CBF PET images, with reference to the semiautomatically coregistered PET/MR fused images (Fig. 1). The same ROIs were placed on other functional images as well. In the rat models of left MCA occlusion, oval ROIs were placed on the bilateral MCA territories and compared between the ipsilateral and contralateral sides.

RESULTS

Figure 2A shows the PET images of a spheric phantom filled with $H_2{}^{15}O$ water for the evaluation of partial-volume effect. The count ratios were 0.36, 0.54, 0.73, and 0.89 for spheres measuring 10, 13, 17, and 22 mm in diameter, respectively, as compared with the count for 28-mm spheres, which provided full recovery (Fig. 2B). Because the brain volume of rats corresponds to that of 15-mm spheres, the partial-volume effect for the whole brain was calculated as 0.7. Figure 3A shows a coronal PET image of the rat brain after $^{15}O_2$ inhalation during the steady state. The profile curves of radioactivity at the line passing the basal ganglia are illustrated with and without attenuation correction in Figure 3B. The profile curves with and without attenuation correction were identical. Figure 4 shows the coronal images of a lung phantom placed in the pleural cavity of a sacrificed rat ventilated with $^{15}O_2$ gas. High radioactivity was found in the pleural cavities bilaterally. No radioactivity from the lung phantom was detected in the brain, indicating that the effect of scatter events from the lung was small. Figure 5 shows a plot of the radioactivity (cps/g) concentrations against the sample volumes of the $H_2{}^{15}O$ solution by well counter. The radioactivity was constant for volumes in the range of 0.025–0.20 mL.

The mean systolic and diastolic BPs, PaO_2, $PaCO_2$, hemoglobin concentration, hematocrit, and SaO_2 are summarized in Table 1. The BP remained stable during the PET measurements.

The total time taken for the entire PET scan in each rat was 73.3 ± 5.8 (68–85) min. In both the ^{15}O-CO_2 and ^{15}O-O_2 studies, the radioactivity count in the brain reached a steady state approximately 10 min after continuous ^{15}O gas inhalation (Fig. 6).

Quantitative PET data in the entire brain were as follows: CBF, 32.3 ± 4.5 mL/100 mL/min; $CMRO_2$, 3.23 ± 0.42 mL/100 mL/min; OEF, 64.6% ± 9.1%; and CBV, 5.05 ± 0.45 mL/100 mL. Functional images of the CBF, $CMRO_2$, OEF, and CBV are shown in Figure 7.

For the findings in the rat model of left MCA occlusion, both rats showed decreased CBF and $CMRO_2$ in the ipsilateral MCA territory, and one of the rats showed increased OEF in the ipsilateral MCA territory. Quantitative values in the ipsilateral and contralateral MCA territories were as follows: CBF, 18.6/30.8 mL/100 mL/min; OEF, 74.3%/65.4%; and $CMRO_2$, 1.79/2.64 mL/100 mL/min.

DISCUSSION

We have reported a method to measure the CBF, CBV, OEF, and $CMRO_2$ in the brain of anesthetized rats by PET, according to the original ^{15}O-CO_2 and ^{15}O-O_2 steady-state inhalation technique combined with ^{15}O-CO inhalation. The methodology in this study is the same as the steady-state method used in clinical PET examinations (*10–12*).

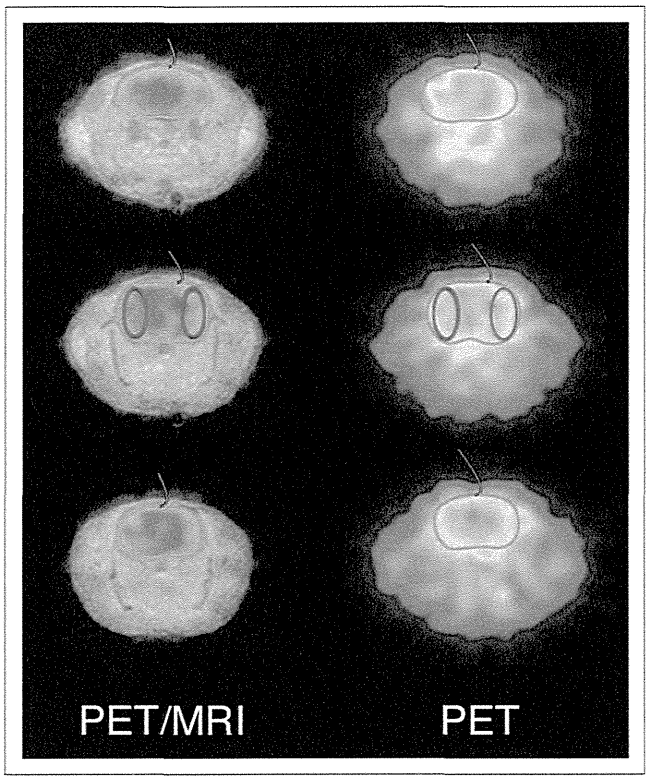

FIGURE 1. Location of ROIs on whole-brain PET slice at maximal cross-section and adjacent cranial and caudal slices. Green ROI = whole brain; red ROI = MCA territories.

Yee et al. performed tracheal administration of ^{15}O-O_2 gas through a surgically placed airway tube in anesthetized rats (*3*). The ^{15}O-O_2 was stored in a syringe (74–111 MBq, 5 cm^3) and insufflated into the lung. Their study indicated that ^{15}O-O_2 administration through the trachea did not affect the image quality of the brain. Tracheotomy also had no significant influence on the physiologic conditions of the rats during the experiments. In our method, one end of the airway tube was inserted into the trachea after tracheotomy and fixed tightly to avoid leakage of the ^{15}O gases. The other end of the airway tube was connected to the ventilator, which continuously supplied the ^{15}O gases at a controlled rate of radioactivity. As shown in Figure 4, no radioactivity in the brain was detected during the ^{15}O-gas insufflation to the balloon phantoms located in the chest cavity. The present PET data acquisition in the 2-D mode was less sensitive to scatter events than acquisitions in the 3-dimensional mode. Quantitative measurement in 3-dimensional mode clinical PET can be achieved with proper scatter correction, just as in the 2-D mode (*18*). We intend to quantitatively measure ^{15}O gas in a 3-dimensional-mode small-animal PET study in the near future.

It is essential, in the ^{15}O gas steady-state inhalation method, to stabilize the radioactivity of the inhaled gases. Artificial ventilation was performed with a radioactive gas stabilization system in this study. The radioactivity distribution in the brain became stable by approximately 10 min after the start of the ^{15}O-CO_2 and ^{15}O-O_2 inhalation. There was a slight increase even after 10 min. The average increase of the count from 10 to 15 min was 3.4% in the CO_2 study and 3.7% in the O_2 study. These increases were relatively small as compared with the average variability in brain counts between 10 and 15 min (5.5%). We performed an experimental study for continuous monitoring of arterial BP in 3 rats. Systemic BP had been generally stable from 15 to 90 min after the start of anesthesia (data not shown). The biologic half-life of xylazine is 2–3 h in rats, which is sufficiently long to maintain a stable condition during the PET measurements.

In this study, 2 rats underwent ^{15}O-O_2 scanning before ^{15}O-CO_2 scanning, and the other rats were scanned in the opposite order. No systematic changes in CBF, OEF, or $CMRO_2$ dependent on the order of scanning were observed.

The whole-body blood volume of the rats weighing about 300 g was estimated to be about 17 mL (*19*). Sampling of a large amount of blood may affect the physiologic condition of the rats. In the present study, only 0.2 mL of arterial blood was taken at each measurement, and the total volume of blood withdrawn was 0.5 mL. This volume was much smaller than that reported in previous studies (*9,20*). The small-volume sampling in this study was considered to have a negligible influence on systemic circulation.

We measured the radioactivity of whole blood and plasma, weighing around 0.025 g, by well counter to examine the volume dependency of the radioactivity count. It was confirmed that the measurement was accurate and that reproducibility was feasible for 0.025-g samples.

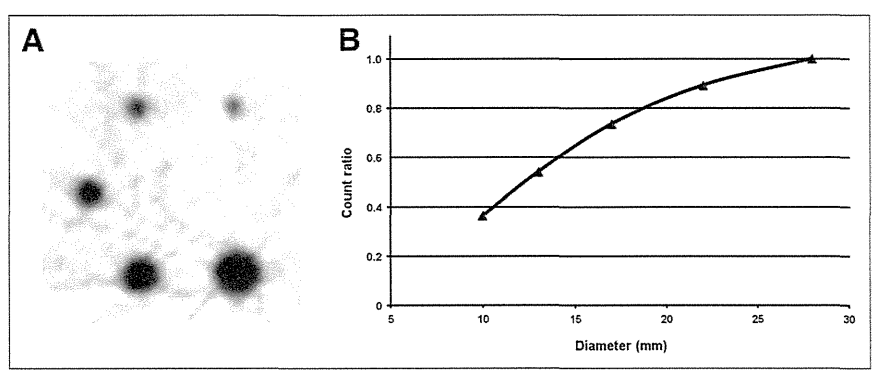

FIGURE 2. PET image of NEMA phantom (A) and curve constructed by plotting mean count ratios against sphere diameters (B).

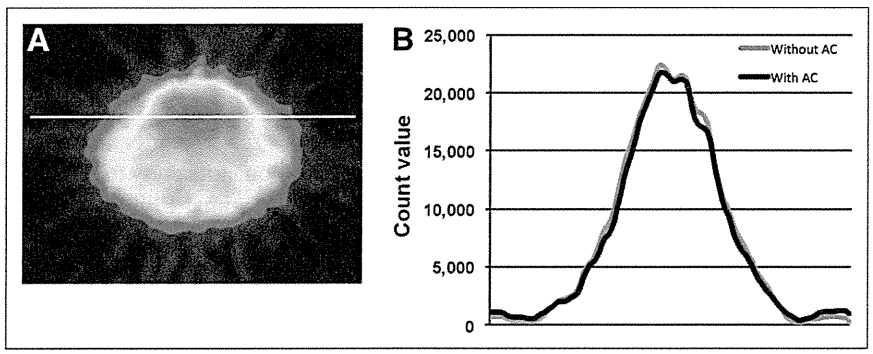

FIGURE 3. ^{15}O-O_2 PET image of brain (white line indicates location of profile curves) (A) and profile curves of brain with and without attenuation correction (B). AC = attenuation correction.

In previous studies, tissue attenuation of ^{15}O was corrected by means of transmission data acquired using the external rod source of ^{68}Ge–^{68}Ga (*9*). The scan duration ranged from 30 to 60 min. When we performed a transmission scan, the duration of the total PET experiment almost doubled from 70 to 130 min. Furthermore, making tissue attenuation maps of small animals using a clinical PET device increases transmission bias and noise because of the large ring diameter. Underestimation by 4% was observed in the experimental study of a rat phantom of 3-cm diameter without attenuation correction, as reported in the previous study (*21*). Scatter fraction in the 2D mode was 13% in the human study according to the performance of our PET scanner (*13*). In our study, we could not perform attenuation and scatter correction because of the limitation of the PET scanner. However, we confirmed from our experimental studies that the tissue attenuation in the rat head and the scatter fraction from outside the brain were small. The fact that attenuation and scatter correction needed to be performed to improve the accuracy was a limitation of our study.

We monitored the systemic BP, body temperature, heart rate, hemoglobin concentration, $PaCO_2$, PaO_2, and SaO_2. Among these parameters, the PaO_2 (56.3 ± 9.3 mm Hg) was unexpectedly lower than the physiologic range and variable, compared with the other physiologic measurements. One possible reason was the slightly reduced oxygen concentration of the inhaled gas. The oxygen concentration of the gas from the radioactive gas stabilization system was 18.1% in ^{15}O-O_2 gas studies. In the target box for ^{15}O-O_2 production, the concentration ratio of cold O_2 to N_2 was 0.5%/99.5%. The ^{15}O-O_2 gas with N_2 gas from the target box was transferred to the gas stabilizer system, and room air was mixed with the ^{15}O-O_2 gas while radioactivity concentration was adjusted. As a result, the oxygen concentration of the inhaled gas was lower than that of the room air because of the addition of the target gas, in which the main component was N_2 gas. Another reason was the effect of the anesthesia used in this study. Reduction in the PaO_2 after the administration of butorphanol, buprenorphine, and midazolam was reported from a previous rabbit study, and this effect was sustained for about 2 h (*22*). High variability in the PaO_2 was probably due to the differences in individual reactions to the anesthesia. To maintain physiologic conditions and reduce the variability, the constitution of the inhaled gas should be readjusted by the addition of O_2.

In previous PET studies, a bolus injection of ^{15}O-labeled water (^{15}O-H_2O) was used for quantitative measurement of the CBF; the reported CBF values ranged from 35 to 51 mL/100 g/min (*6,8,20*). Kobayashi et al. reported a steady-state method consisting of a bolus injection followed by injection of ^{15}O-H_2O at slowly increasing doses with a multiprogramming syringe pump (*9*). The CBF value under chloral hydrate anesthesia was 49.2 ± 5.4 mL/100 g/min. The CBF value measured in our study was much smaller than these previously reported values. The first possible reason is underestimation due to the partial-volume effect. We used a clinical PET device with a larger spatial resolution (4.0 mm in FWHM). According to the phantom study, this underestimation was by approximately 70%, because the diameter of the rat brain is about 15 mm. The radioactivity

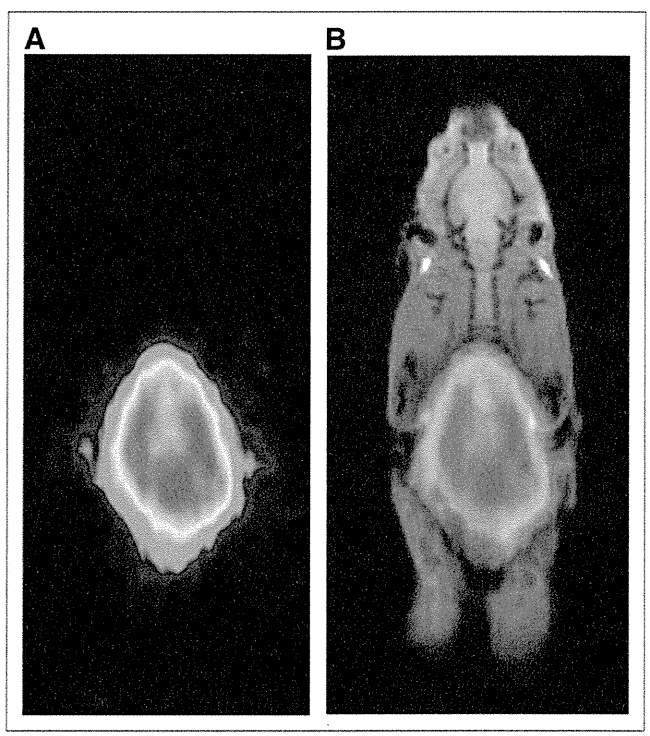

FIGURE 4. Coronal PET (A) and PET/MR (B) images of lung phantom ventilated with ^{15}O-O_2 gas.

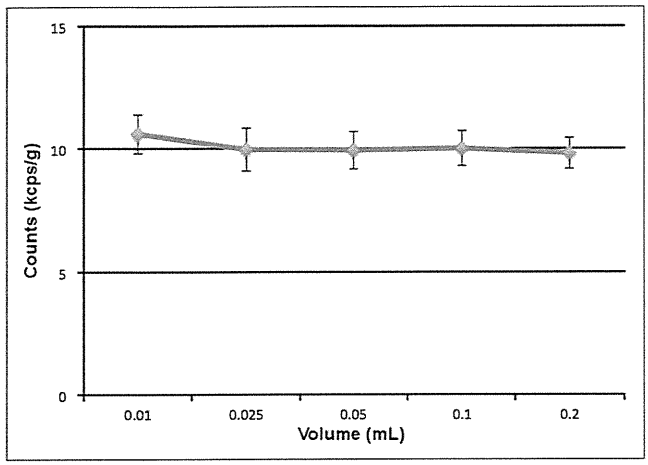

FIGURE 5. Relationship between radioactivity (kcps/g) and sample volume of $H_2{}^{15}O$ solution by well counter.

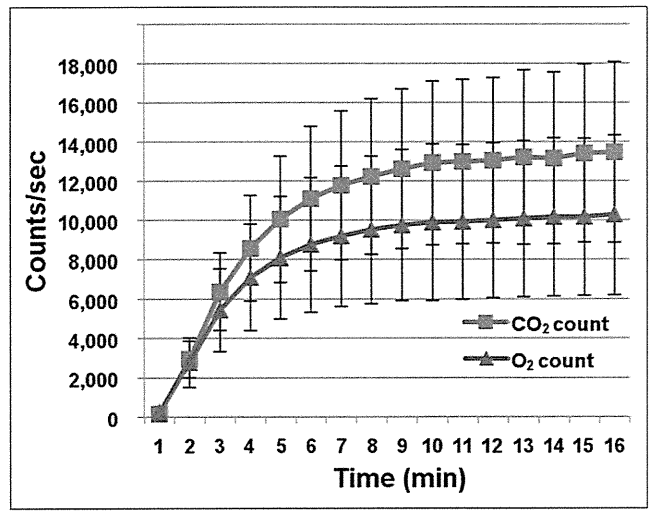

FIGURE 6. Time–activity curves in brain during continuous inhalation of ^{15}O-CO_2 and ^{15}O-O_2 gas. cps = count/s.

count in the brain was divided by 0.70 to correct the partial-volume effect for full count recovery. This corrected count was substituted for C_t in the following equation described in the "Methods" section: regional CBF = $\lambda/(C_a/C_t - 1/\rho)$. After correction for the partial-volume effect, we obtained a whole-brain CBF value of approximately 84 mL/100 mL/min, which is in agreement with the values obtained by the autoradiographic method (*16*) and the Kety–Schmidt method (*23,24*), the results of which are not influenced by the partial-volume effect. The second possible reason is the influence of anesthesia. Most previous studies used chloral hydrate, which is difficult to use because of its narrow margin of safety and lack of analgesic effect. The different anesthetic technique used might also have produced the differences in the results. The third reason is the influence of $PaCO_2$ on the CBF. Hypocapnia causes reduction of the global CBF in the rat under isoflurane or halothane anesthesia (*25*). On the basis of studies using the steady-state method, Kobayashi et al. reported that the CBF was 49.2 ± 5.4 mL/100 g/min when the $PaCO_2$ was 49.7 ± 3.9 mm Hg (*9*). In this study, the CBF was 32.3 ± 4.5 mL/100 mL/min when the $PaCO_2$ was 36.6 ± 1.6 mm Hg. The lower CBF value in the present study was partly due to the lower $PaCO_2$ levels. Another possible reason is that systemic underestimation by the steady-state inhalation method, compared with that in the bolus injection method, was partly due to the tissue heterogeneity between the gray and white matter (*26*).

TABLE 1
BP, HR, and Arterial Blood Gas Data During PET Measurement

Parameter	Mean ± SD
BP (mm Hg) (n = 4)	
Systolic	106 ± 4
Diastolic	79 ± 5
HR (bpm) (n = 4)	326 ± 20
pH	7.45 ± 0.03
$PaCO_2$ (mm Hg)	36.6 ± 1.6
PaO_2 (mm Hg)	56.3 ± 9.3
SaO_2 (%)	89.3 ± 3.7

Few PET studies have reported measurement of OEF. Reported values of OEF in rats under pentobarbital anesthesia are 54% ± 11% using the kinetic method with injectable ^{15}O-O_2 and 57% ± 13% using the surgical method based on the arterial–venous difference in oxygen concentration (*4,20*). Other studies using ^{15}O-O_2 hemoglobin–containing liposome vesicles reported OEF values in rats under chloral hydrate anesthesia of 61% ± 16% (6) and 56% ± 4% (*27*). OEF is a function of the ^{15}O-O_2/^{15}O-CO_2 count ratio. OEF is not significantly affected by the partial-volume effect, because the calculation involves canceling out by dividing the ^{15}O-O_2 count by the ^{15}O-CO_2 count in the brain tissue. The OEF value calculated in our study was a little higher than the previously reported values. The OEF values reported from other studies were also higher than those reported from human studies. The OEF values were 54%–61% in the normal rat study but only 44% in a normal human study (*28*). Previous studies reported higher OEF values in monkeys (54% ± 6%) and pigs (59% ± 9%) (*29,30*). Therefore, differences among species might be the reason for the high OEF in the rats in the present study. OEF elevation was observed in the MCA occlusion model, as in the human brain in our study. The OEF values were 74.3% and 65.4% in the ipsilateral and contralateral MCA territories, respectively. The capacity to adapt to flow decreases was observed in rats, just as in humans.

Yee et al. reported quantitative measurement of $CMRO_2$ in the rat brain with briefly inhaled ^{15}O-labeled oxygen gas (*3*). The measured $CMRO_2$ value under α-chloralose anesthesia was 6.65 ± 0.48 mL/100 g/min. Temma et al. used an artificial lung to dissolve ^{15}O-O_2 in the blood and reported a $CMRO_2$ value of 4.3 ± 1.3 mL/100 g/min under pentobarbital anesthesia (*20*). Another group used hemoglobin-containing liposome vesicles or liposome-encapsulated hemoglobin with ^{15}O-O_2 and reported $CMRO_2$ values of 6.8 ± 1.4 (under chloral

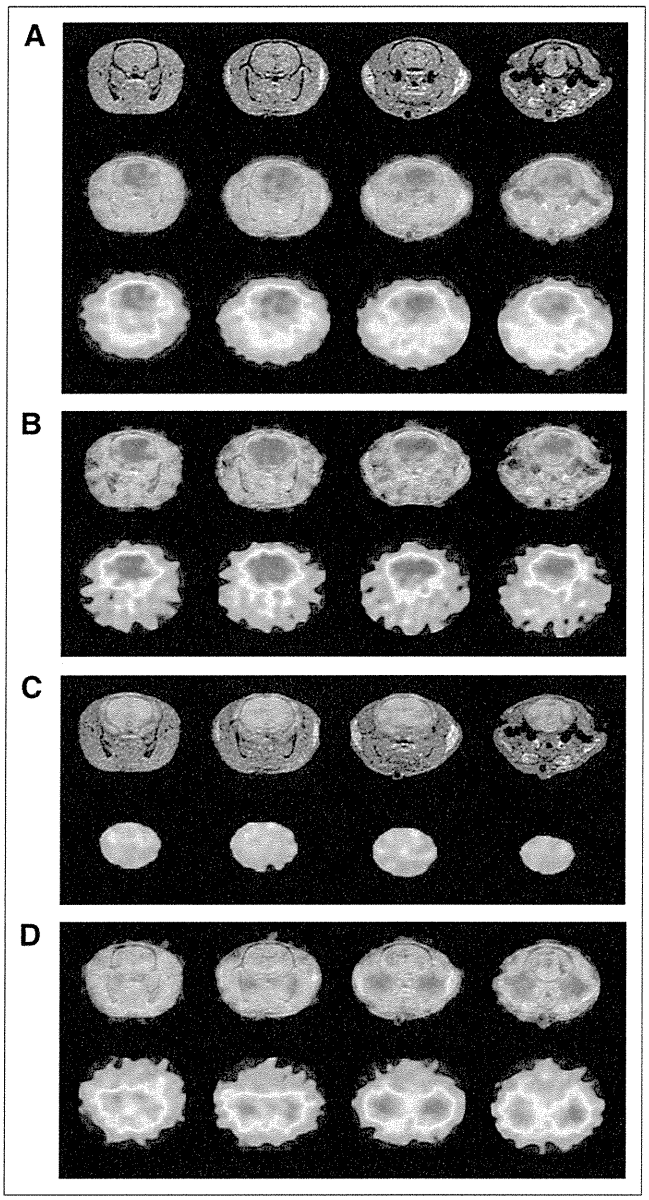

FIGURE 7. MR (upper), PET/MR fusion (middle), and PET (lower) images of CBF (A). PET/MR fusion (upper) and PET (lower) images of CMRO2 (B), OEF (C), and CBV (D). Images in same column indicate same transaxial cross-section of brain (A–D).

hydrate anesthesia) and 4.8 ± 0.2 mL/100 g/min (under ketamine and xylazine anesthesia), respectively (*6,7*). Kobayashi et al. recently reported a $CMRO_2$ value of 6.2 ± 0.4 mL/100 g/min under chloral hydrate anesthesia as measured by the steady-state method with injection of $^{15}O_2$ hemoglobin–containing vesicles (*27*). The $CMRO_2$ value measured in our study (3.23 ± 0.42 mL/100 mL/min) was smaller than these previously reported values. However, after correction for the partial-volume effect, the $CMRO_2$ was approximately 8.4 mL/100 mL/min, which is in agreement with the values (10.3 and 7.57 mL/100 mL/min) obtained by the method of Kety and Schmidt (*23,24*).

There have been no reports of measurement of the CBV in the rat brain by ^{15}O-CO gas inhalation PET. This study evaluated all PET parameters (CBF, $CMRO_2$, OEF, and CBV) by ^{15}O-labeled gases with correction for intravascular hemoglobin-bound $^{15}O_2$. Kobayashi reported a mean value of the CBV of 4.9 ± 0.4 mL/100 g as measured by injection of ^{15}O-CO hemoglobin–containing vesicles, consistent with the result of our study (*27*). The small-vessel–to–large-vessel hematocrit ratio in the rat brain has been fixed at 0.70 (*17*); this ratio was shown to have little effect on the OEF or $CMRO_2$ values. When we used 0.85 as the value of the hematocrit ratio (a value often used in clinical studies), the $CMRO_2$ and OEF increased by approximately 1% (data not shown).

Quantitative PET measurement in a rat model of unilateral MCA occlusion was performed as an experimental study. A decrease in both the CBF and the $CMRO_2$ and an increase in the OEF were detected in the ipsilateral MCA territory (data not shown). We concluded that evaluation in an ischemia model is feasible with this PET technique.

CONCLUSION

Although further improvements of the gas inhalation system may be needed, we demonstrated the feasibility of quantitative measurements of CBF, CBV, $CMRO_2$, and OEF using PET according to the original steady-state inhalation method of ^{15}O-CO_2 and ^{15}O-O_2 gas and the CBV measurement by ^{15}O-CO gas inhalation in normal rats under anesthesia.

DISCLOSURE

The costs of publication of this article were defrayed in part by the payment of page charges. Therefore, and solely to indicate this fact, this article is hereby marked "advertisement" in accordance with 18 USC section 1734. This study was partly supported by the Molecular Imaging Program, a grant (no. 21591561) from the Ministry of Education, Culture, Sports, Science, and Technology (MEXT), Japan. No other potential conflict of interest relevant to this article was reported.

REFERENCES

1. Fox PT, Mintun MA, Raichle ME, Miezin FM, Allman JM, Van Essen DC. Mapping human visual cortex with positron emission tomography. *Nature.* 1986;323:806–809.
2. Powers WJ, Clarke WR, Grubb RL Jr, Videen TO, Adams HP Jr, Derdeyn CP. Extracranial-intracranial bypass surgery for stroke prevention in hemodynamic cerebral ischemia: the Carotid Occlusion Surgery Study randomized trial. *JAMA.* 2011;306:1983–1992.
3. Yee SH, Lee K, Jerabek PA, Fox PT. Quantitative measurement of oxygen metabolic rate in the rat brain using microPET imaging of briefly inhaled ^{15}O-labelled oxygen gas. *Nucl Med Commun.* 2006;27:573–581.
4. Magata Y, Temma T, Iida H, et al. Development of injectable O-15 oxygen and estimation of rat OEF. *J Cereb Blood Flow Metab.* 2003;23:671–676.
5. Temma T, Magata Y, Kuge Y, et al. Estimation of oxygen metabolism in a rat model of permanent ischemia using positron emission tomography with injectable15O-O2. *J Cereb Blood Flow Metab.* 2006;26:1577–1583.
6. Tiwari VN, Kiyono Y, Kobayashi M, et al. Automatic labeling method for injectable ^{15}O-oxygen using hemoglobin-containing liposome vesicles and its application for measurement of brain oxygen consumption by PET. *Nucl Med Biol.* 2010;37:77–83.
7. Awasthi V, Yee SH, Jerabek P, Goins B, Phillips WT. Cerebral oxygen delivery by liposome-encapsulated hemoglobin: a positron-emission tomographic evaluation in a rat model of hemorrhagic shock. *J Appl Physiol.* 2007;103:28–38.

8. Weber B, Spath N, Wyss M, et al. Quantitative cerebral blood flow measurements in the rat using a beta-probe and H2 ^{15}O. *J Cereb Blood Flow Metab.* 2003; 23:1455–1460.
9. Kobayashi M, Kiyono Y, Maruyama R, Mori T, Kawai K, Okazawa H. Development of an $H_2{}^{15}O$ steady-state method combining a bolus and slow increasing injection with a multiprogramming syringe pump. *J Cereb Blood Flow Metab.* 2011;31:527–534.
10. Jones T, Chesler DA, Ter-Pogossian MM. The continuous inhalation of oxygen-15 for assessing regional oxygen extraction in the brain of man. *Br J Radiol.* 1976; 49:339–343.
11. Frackowiak RS, Lenzi GL, Jones T, Heather JD. Quantitative measurement of regional cerebral blood flow and oxygen metabolism in man using ^{15}O and positron emission tomography: theory, procedure, and normal values. *J Comput Assist Tomogr.* 1980;4:727–736.
12. Lammertsma AA, Jones T. Correction for the presence of intravascular oxygen-15 in the steady-state technique for measuring regional oxygen extraction ratio in the brain: 1. Description of the method. *J Cereb Blood Flow Metab.* 1983;3:416–424.
13. Iida H, Miura S, Kanno I, Ogawa T, Uemura K. A new PET camera for non-invasive quantitation of physiological functional parametric images: Headtome-V-Dual. In: Myers R, Cunningham V, Bailey D, Jones T, eds. *Quantitation of Brain Function Using PET.* San Diego, CA: Academic Press; 1996:57–61
14. Yamamoto S, Imaizumi M, Kanai Y, et al. Design and performance from an integrated PET/MRI system for small animals. *Ann Nucl Med.* 2010;24:89–98.
15. Shimamura N, Matchett G, Tsubokawa T, Ohkuma H, Zhang J. Comparison of silicon-coated nylon suture to plain nylon suture in the rat middle cerebral artery occlusion model. *J Neurosci Methods.* 2006;156:161–165.
16. Herscovitch P, Raichle ME. What is the correct value for the brain–blood partition coefficient for water? *J Cereb Blood Flow Metab.* 1985;5:65–69.
17. Cremer JE, Seville MP. Regional brain blood flow, blood volume, and haematocrit values in the adult rat. *J Cereb Blood Flow Metab.* 1983;3:254–256.
18. Ibaraki M, Miura S, Shimosegawa E, et al. Quantification of cerebral blood flow and oxygen metabolism with 3-dimensional PET and ^{15}O: validation by comparison with 2-dimensional PET. *J Nucl Med.* 2008;49:50–59.
19. Lee HB, Blaufox MD. Blood volume in the rat. *J Nucl Med.* 1985;26:72–76.
20. Temma T, Kuge Y, Sano K, et al. PET O-15 cerebral blood flow and metabolism after acute stroke in spontaneously hypertensive rats. *Brain Res.* 2008;1212:18–24.
21. Chow PL, Rannou FR, Chatziioannou AF. Attenuation correction for small animal PET tomographs. *Phys Med Biol.* 2005;50:1837–1850.
22. Schroeder CA, Smith LJ. Respiratory rates and arterial blood-gas tensions in healthy rabbits given buprenorphine, butorphanol, midazolam, or their combinations. *J Am Assoc Lab Anim Sci.* 2011;50:205–211.
23. Hägerdal M, Harp J, Nilsson L, Siesjo BK. The effect of induced hypothermia upon oxygen consumption in the rat brain. *J Neurochem.* 1975;24:311–316.
24. Nilsson B, Siesjo BK. A method for determining blood flow and oxygen consumption in the rat brain. *Acta Physiol Scand.* 1976;96:72–82.
25. Young WL, Barkai AI, Prohovnik I, Nelson H, Durkin M. Effect of PaCO2 on cerebral blood flow distribution during halothane compared with isoflurane anaesthesia in the rat. *Br J Anaesth.* 1991;67:440–446.
26. Herscovitch P, Raichle ME. Effect of tissue heterogeneity on the measurement of cerebral blood flow with the equilibrium C15O2 inhalation technique. *J Cereb Blood Flow Metab.* 1983;3:407–415.
27. Kobayashi M, Mori T, Kiyono Y, et al. Cerebral oxygen metabolism of rats using injectable ^{15}O-oxygen with a steady-state method. *J Cereb Blood Flow Metab.* 2012;32:33–40.
28. Ito H, Kanno I, Kato C, et al. Database of normal human cerebral blood flow, cerebral blood volume, cerebral oxygen extraction fraction and cerebral metabolic rate of oxygen measured by positron emission tomography with ^{15}O-labelled carbon dioxide or water, carbon monoxide and oxygen: a multicentre study in Japan. *Eur J Nucl Med Mol Imaging.* 2004;31:635–643.
29. Kudomi N, Hayashi T, Teramoto N, et al. Rapid quantitative measurement of CMRO(2) and CBF by dual administration of (15)O-labeled oxygen and water during a single PET scan-a validation study and error analysis in anesthetized monkeys. *J Cereb Blood Flow Metab.* 2005;25:1209–1224.
30. Mörtberg E, Cumming P, Wiklund L, Rubertsson S. Cerebral metabolic rate of oxygen (CMRO2) in pig brain determined by PET after resuscitation from cardiac arrest. *Resuscitation.* 2009;80:701–706.

Cerebral Blood Flow and Metabolism Measurement Using Positron Emission Tomography before and during Internal Carotid Artery Test Occlusions: Feasibility of Rapid Quantitative Measurement of CBF and OEF/$CMRO_2$

N. KAWAI[1], M. KAWANISHI[1], A. SHINDOU[1], N. KUDOMI[2], Y. YAMAMOTO[3], Y. NISHIYAMA[3], T. TAMIYA[1]

[1] Department of Neurological Surgery, 2Department of Medical Physics, 3Department of Radiology, Faculty of Medicine, Kagawa University; Kagawa, Japan

Key words: balloon test occlusion, cerebral blood flow, cerebral oxygen metabolism, internal carotid artery, positron emission tomography

Summary

Balloon test occlusion (BTO) of the internal carotid artery (ICA) combined with cerebral blood flow (CBF) study is a sensitive test for predicting the outcome of permanent ICA occlusion. However, false negative results sometimes occur using single photon emission tomography (SPECT). We have recently developed a rapid positron emission tomography (PET) protocol that measures not only the CBF but also the cerebral oxygen metabolism before and during BTO in succession. We measured acute changes in regional CBF and OEF/CMRO2 before and during BTO in three cases with large or giant cerebral aneurysms using the rapid PET protocol.

Although no patients showed ischemic symptoms during BTO, PET studies exhibited mildly to moderately decreased CBF (9~34%) compared to the values obtained before BTO in all cases. The average OEF during BTO was significantly increased (21% and 43%) than that of before BTO in two cases. The two cases were considered to be non-tolerant for permanent ICA occlusion and treated without ICA sacrifice.

Measurement of the CBF and OEF/CMRO2 using a rapid PET protocol before and during BTO is feasible and can be used for accurate assessment of tolerance prediction in ICA occlusion.

Introduction

Occlusion of the ICA is sometimes necessary to treat giant ICA aneurysms and tumors encasing the ICA. The consequences of ICA occlusion range from no symptoms to devastating hemispheric strokes [1]. The balloon test occlusion (BTO) of the ICA has been used to predict whether a patient can tolerate temporary or permanent occlusion of the ICA. If the patient develops any sign of hemispheric ischemia during BTO, permanent ICA occlusion should not be performed or an extracranial-intracranial (EC-IC) bypass is considered before ICA occlusion [2]. However, BTO with neurological evaluation alone has a high false negative rate [3]. To improve the sensitivity, several reports have proposed CBF measurement to predict the likelihood of ischemic complications following ICA occlusion during BTO [4-10]. Single photon emission tomography (SPECT) allows semi-quantitative determination of the CBF through-

A

Before BTO

During BTO

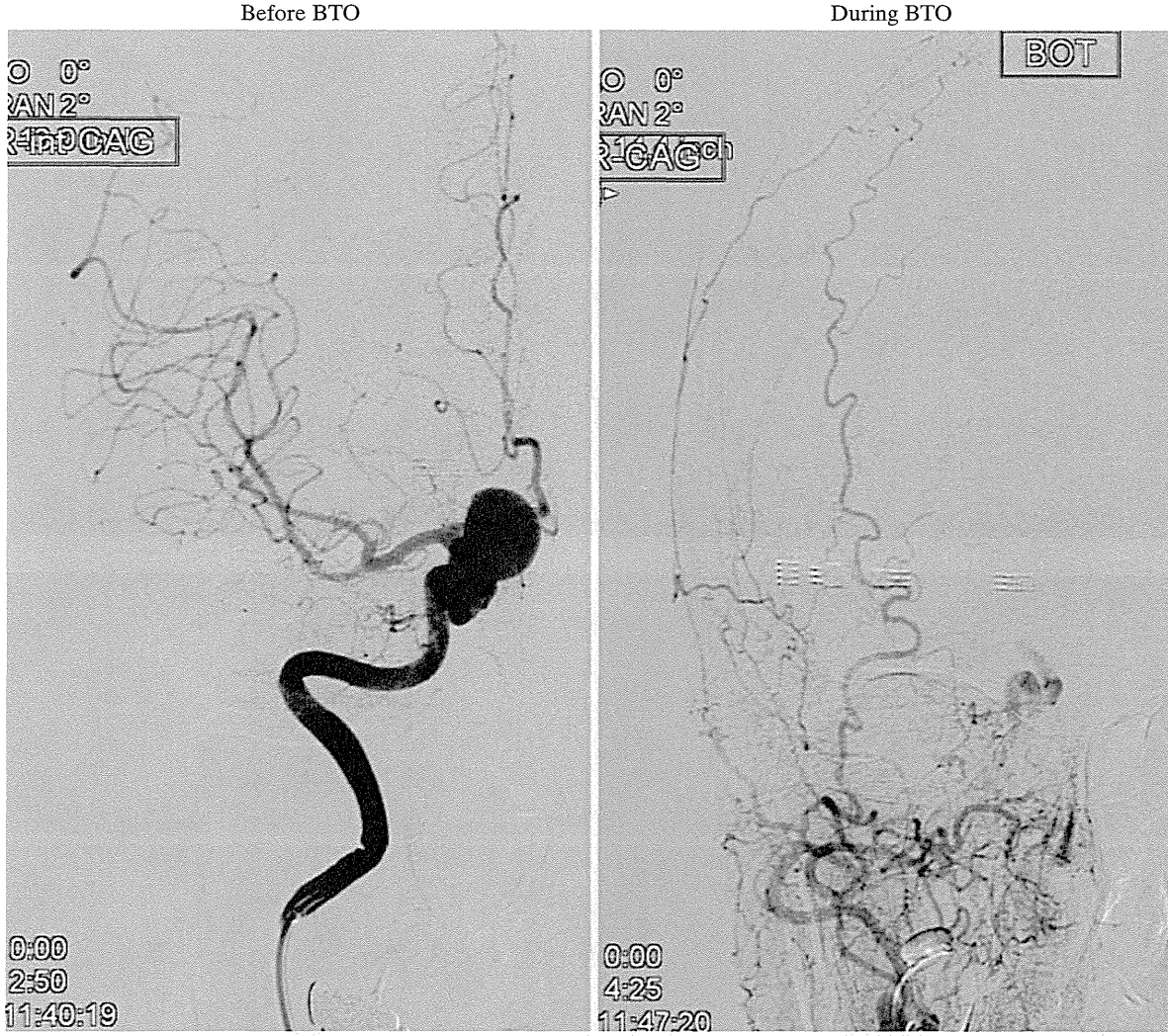

Rt. CAG

Rt. CAG

B

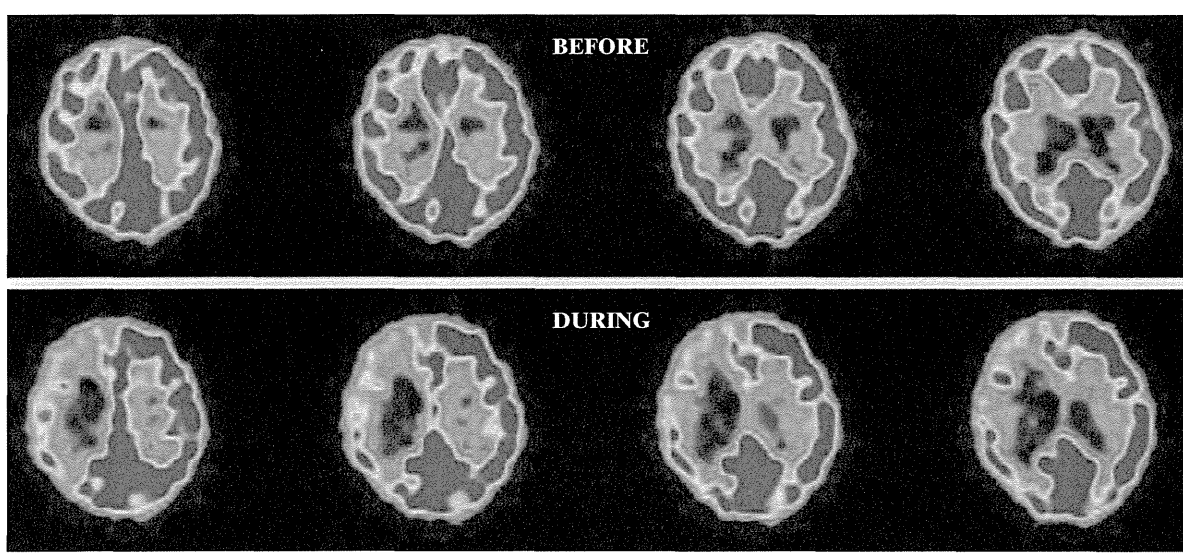

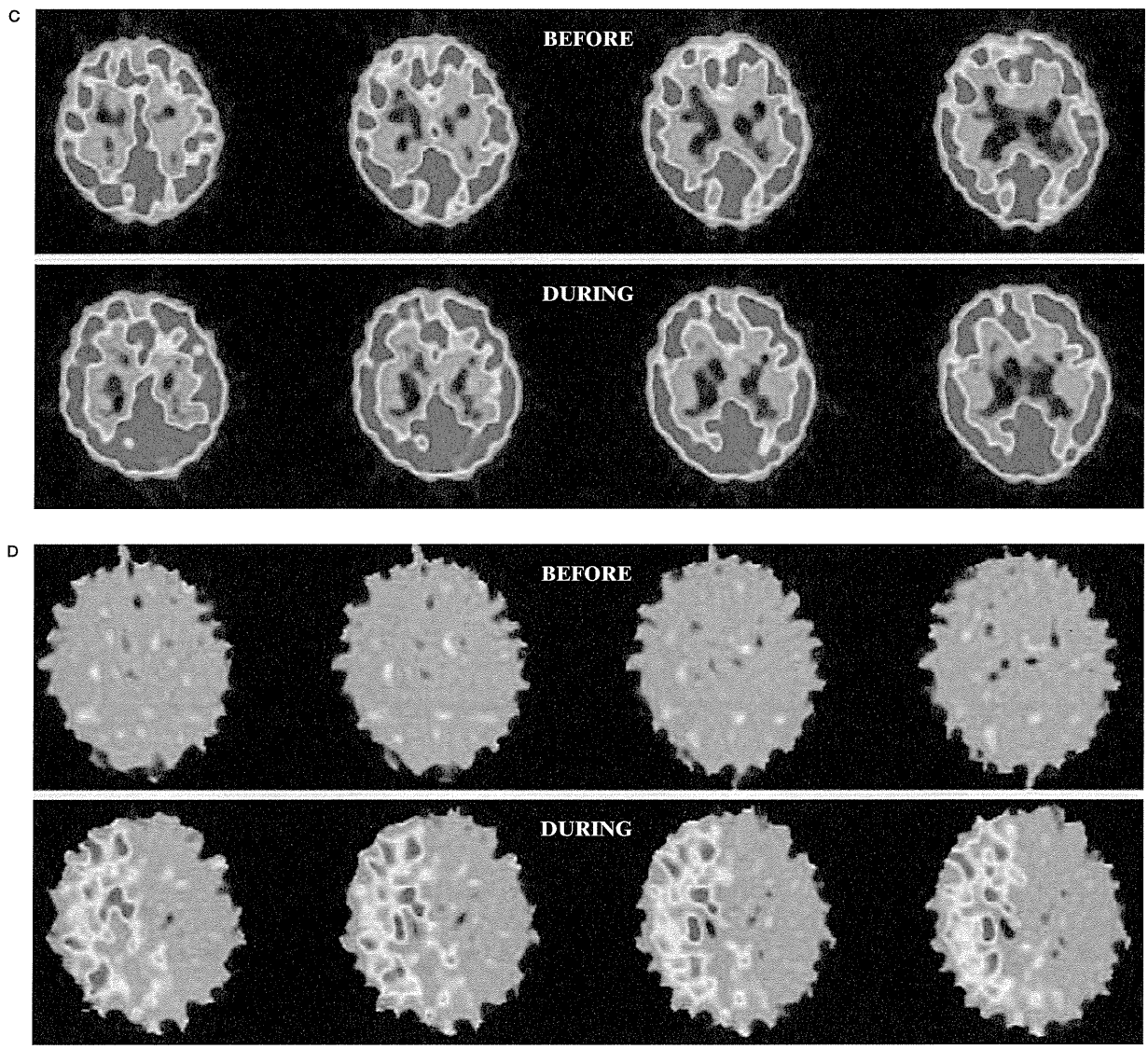

Figure 1 A) Right ICA angiogram shows a large paraclinoid aneurysm. The right ICA is completely occluded by a balloon during BTO. B) During BTO of the right ICA, a moderate decrease in CBF in the right MCA territory is demonstrated by PET study. The $CMRO_2$ was symmetrical (C) and the OEF in the right MCA territory is markedly increased (D). This patient was considered to be non-tolerant for permanent ICA occlusion.

out the entire brain and is reported to be useful for evaluating collateral blood flow after permanent ICA occlusion [4,6,8]. However, up to 20% of the patients did not tolerate ICA sacrifice, even though they had symmetrical SPECT scans during BTO [11,12]. Besides the CBF, oxygen extraction fraction (OEF) and cerebral metabolic rate of oxygen ($CMRO_2$), which can be obtained only with positron emission tomography (PET) study, provide us important indices for assessing ischemic degree [13-15]. However, the complex nature of the PET procedure and its relatively long protocol limit the applicability of PET study to BTO. One of our colleagues developed a new dual tracer autoradiographic (DRAG) method to shorten PET examination time [16,17]. This method enabled us to measure the CBF and OEF/$CMRO_2$ values before and during BTO in succession. In this manuscript, we report initial three cases of PET study for evaluating the cerebral blood flow and metabolism before and during BTO, especially describing the feasibility of rapid quantitative measurement of the CBF and OEF/$CMRO_2$.

Materials and Methods

Three women with large or giant cerebral aneurysms involving the ICA underwent BTO to evaluate brain tolerance to sacrifice the ICA. Written informed consent was obtained from all patients after a detailed explanation of the test procedure.

Balloon test occlusion

After diagnostic cerebral angiography, a 5-French double-lumen balloon catheter was inserted into the ICA of the affected side with systemic heparinization (5,000-10,000 IU). One lumen is used to inflate the balloon, and the central lumen is a distal lumen beyond the balloon connecting to a pressure transducer. Cross-filling via the communicating arteries was examined by contralateral carotid angiogram or vertebral angiogram under balloon inflation of the objective carotid artery. A trial BTO was performed for 15 min to examine neurological signs or changes in the stump pressure. Complete occlusion of the ICA was confirmed by a sudden drop in the stump pressure and contrast injection. After trial BTO, patients were transferred from the angiography suite to the radioisotope suite with the balloon deflated but still in place under frequent monitoring of the activated coagulation time. An adhesive strip was affixed to the catheter at the location of the catheter entrance into the sheath so that it could later be inflated during PET scanning without the use of fluoroscopy.

PET examination

PET acquisition was performed in 2D mode using an ECAT HR+ scanner (Siemens-CTI, Knoxville, USA), which provided 63 tomographic slice images for an axial field-of-view of approximately 150 mm. A five-minute transmission scan using a ^{68}Ge rod source was conducted to correct tissue attenuation. Intermittent arterial blood sampling and radioactivity concentration measurements were performed throughout PET scanning using a catheter implanted in the brachial artery to obtain the arterial input function using an auto well gamma counter (ARC-400, Aloka, Tokyo, Japan). Arterial blood samples were also used to measure hematocrit and blood gas tensions.

In the radioisotope suite, the patients were positioned on a table for the PET camera. First, baseline measurements of CBF and OEF/CMRO2 were performed without balloon inflation. The PET protocol was originally developed as the DRAG method [16,17], in which $^{15}O_2$ and $H_2{}^{15}O$ (or $C^{15}O_2$) are sequentially administered during a single PET scanning to measure the OEF/$CMRO_2$ and CBF. The method was further improved by eliminating the need for CBV data so that the total scan time is shortened to less than 15 min [17]. In the present study, we applied the method by administering firstly $^{15}O_2$ (3000 MBq/min) followed by $C^{15}O_2$ (500 MBq/min) after ten minutes during a single PET scanning (10 s × 6; 20 s × 6; 30 s × 4; 120 s × 3; 5 s × 12; 10 s × 9). The arterial input function was determined by frequent arterial sampling during the PET scanning. After the baseline measurement, the balloon was inflated after sufficient time for eliminating the tracer. Complete occlusion of the ICA was confirmed by a sudden drop in the stump pressure. The ICA was occluded for 15 minutes for the BTO PET study and CBF and OEF/CMRO2 values were measured during BTO. Total examination time in the radioisotope suite was about 50 minutes. Several circular regions of interest (ROI) were placed on CBF images in the middle cerebral artery (MCA) territory. The size of each ROI was 10 mm in diameter. OEF and $CMRO_2$ values were extracted from the same ROIs on CBF images.

Results

None of the three patients exhibited neurologic symptoms during BTO in the angiography suite. Physiological parameters including blood pressure and blood gas tensions were within normal range and were not significantly different between before and during BTO PET examinations.

Case 1

A 66-year-old woman was admitted to our hospital with left upper-quadrant homonymous hemianopsia. Right ICA angiogram demonstrated a large paraclinoid aneurysm (16 × 12 mm) (Figure 1A). The average CBF in the right MCA territory during BTO was 38.4 ml/100 g/min, which was 34% lower than that of before BTO (57.9 ml/100 g/ min) and 35% lower compared to the contralateral value (58.8 ml/100 g/ min) (Figure 1B). The average $CMRO^2$ in the right MCA territory during BTO (4.9 ml/100 g/

min) was slightly higher than that of before BTO (4.5 ml/100 g/min) (Figure 1C). The average OEF in the right MCA territory during BTO was 0.66, which was 43% higher than that of before BTO (0.46) (Figure 1D). This patient was considered to be non-tolerant for permanent ICA occlusion and treated with successful neck clipping.

Case 2

A 50-year-old woman was admitted to our hospital with an incidentally found cerebral aneurysm. Left ICA angiogram demonstrated a large paraclinoid aneurysm (16 × 14 mm) (Figure 2A). BTO resulted in mild global reduction of CBF in the bilateral hemispheres. The average CBF in the left MCA territory during BTO was 41.2 ml/100 g/min, which was 13% lower than that of before BTO (47.0 ml/100 g/ min) and 15% lower compared to the contralateral value (48.6 ml/100 g/ min) (Figure 2B). The average $CMRO_2$ in the left MCA territory during BTO (3.8 ml/100 g/min) was slightly higher than that of before BTO (3.3 ml/100 g/min) (Figure 2C). The average OEF in the left MCA territory during BTO was 0.57, which was 21% higher than that of before BTO (0.47) (Figure 2D). This patient was considered to be non-tolerant for permanent ICA occlusion and treated with successful neck clipping.

Case 3

A 60-year-old woman was admitted to our hospital with right facial numbness and blurred vision. Right ICA angiogram demonstrated a giant cavernous aneurysm (30 × 25 mm) (Figure 3A). BTO resulted in mild global reduction of CBF in the bilateral hemispheres. The average CBF in the right MCA territory during BTO was 46.6 ml/100 g/min, which was 9% lower than that of before BTO (51.0 ml/100 g/ min) and 9% lower compared to the contralateral value (51.5 ml/100 g/ min) (Figure 3B). The average $CMRO^2$ in the right MCA territory during BTO (3.0 ml/100 g/min) was slightly lower than that of before BTO (3.3 ml/100 g/ min) (Figure 3C). The average OEF in the left MCA territory during BTO was 0.51, which was slightly higher than that of before BTO (0.48) (Figure 3D). This patient was considered to be tolerant for permanent ICA occlusion and treated with ICA occlusion without acute or later neurological deficits at six months after the treatment.

Discussion

Occlusion of the ICA was demonstrated to carry 26% risk of ischemia of the ipsilateral hemisphere, of which 46% were fatal, when performed in non-selective patients [3]. Balloon test occlusion (BTO) has been developed as a method to assess the tolerance of permanent ICA occlusion. Linskey et al. reported that the risk of ischemic complications was reduced to 13% by selective carotid occlusion using BTO [3]. However, the appearance of neurological symptoms during BTO exhibited low negative and positive predictive values and was not a good predictor of sustained patient outcome [9]. To improve the sensitivity, various reports have proposed adjunctive methods to predict the likelihood of ischemic complications following ICA occlusion, such as measurement of the stump pressure [4,18] and the CBF [4-10] during BTO.

Measurement of the blood flow has demonstrated that substantial cerebral hypoperfusion occurs even when the patient does not show any neurological signs during BTO and may evaluate a potential risk after the ICA occlusion [19,20]. Among several methods of CBF measurement, SPECT is considered to be the most useful method for evaluating the collateral circulation during BTO [4,6,8]. SPECT images acquired after the completion of BTO reflect the tracer distribution during occlusion when the tracer is injected. Although no definite quantitative criteria are now available to define perfusion abnormalities that may cause cerebral infarction, an interhemispheric difference in tracer uptake less than 10% (CBF ratio < 0.9) is generally accepted to be asymmetric and safe [21]. Palestro et al. [22] reported that the negative predictive value of the symmetric perfusion (CBF ratio > 0.9) during BTO was 100% in 14 patients who underwent carotid occlusion. In the SPECT study, however, up to 20% of the patients did not tolerate ICA sacrifice, even though they had symmetrical SPECT scans during BTO [11,12]. Moreover, a previous study has shown that a considerable reduction in CBF might occur under hypotension after ICA sacrifice, even with negative BTO [23]. It has also been suggested that SPECT asymmetry analysis carries a high rate of false positive test results [6,24], because of the semi-quantitative na-

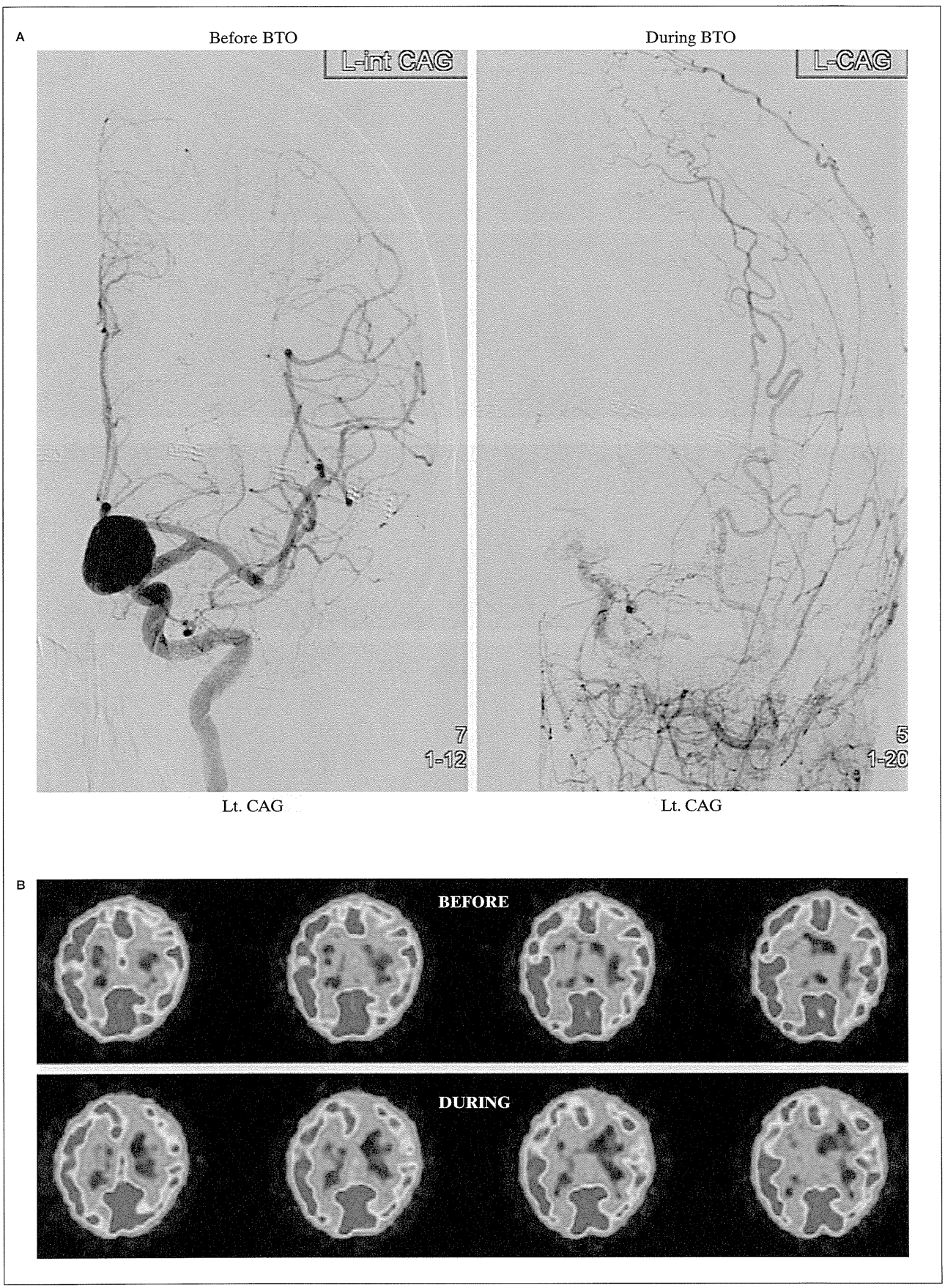
A
Before BTO
During BTO
L-int CAG
L-CAG
7
1-12
5
1-20
Lt. CAG
Lt. CAG
B
BEFORE
DURING

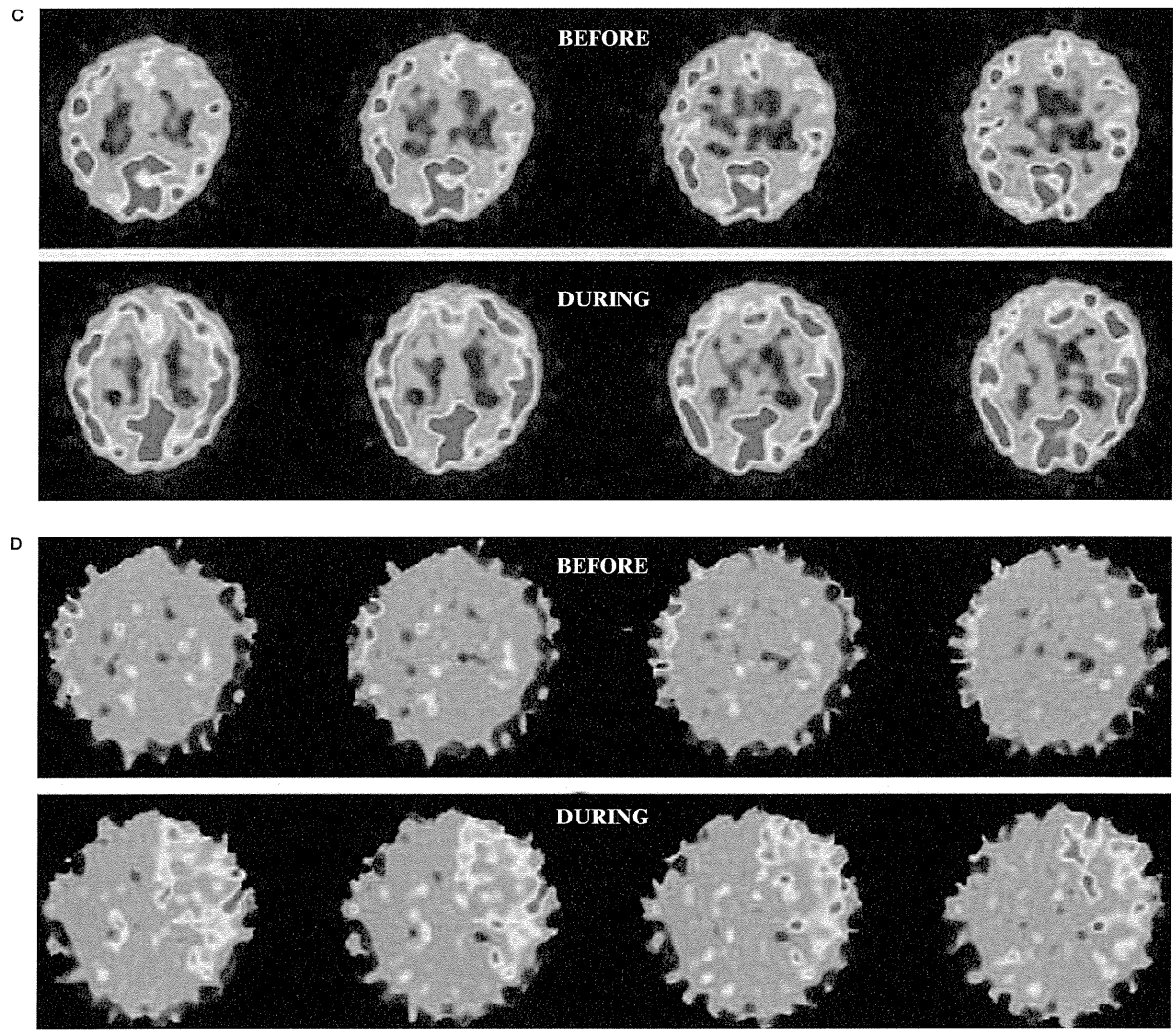

Figure 2 A) Left ICA angiogram shows a large paraclinoid aneurysm. The left ICA is completely occluded by a balloon during BTO. B) During BTO of the left ICA, a mild decrease in CBF in the left MCA territory is demonstrated by PET study. The $CMRO_2$ was symmetrical (C) and the OEF in the left MCA territory is mildly increased (D). This patient was considered to be non-tolerant for permanent ICA occlusion.

ture of the data analysis. The false negative rate of the BTO was lowered to 3-10% by applying quantitative CBF analysis with xenon-enhanced CT [3,25]. They proposed a flow of less than 30 ml/100 g/min as the threshold for occurrence of neurological symptoms after ICA occlusion [3,25]. These results indicate that SPECT asymmetry analysis is not accurate to predict ischemic complications after permanent ICA occlusion and quantitative CBF analysis improves the precision of risk evaluation.

PET study is considered to be the most reliable method for measuring the CBF throughout the entire brain. Besides CBF, CBV, oxygen extraction fraction (OEF) and cerebral metabolic rate of oxygen ($CMRO_2$) provide us with important indices that can be used for assessing the ischemic degree in chronic and acute cerebrovascular disease. In a primate study of cerebral ischemia, $CMRO_2$ not CBF measurement may be the best predictor of reversible or irreversible tissue damage [14,15]. OEF and $CMRO_2$ values provide a true definition of ischemia in patients with aneurysmal subarachnoid hemor-

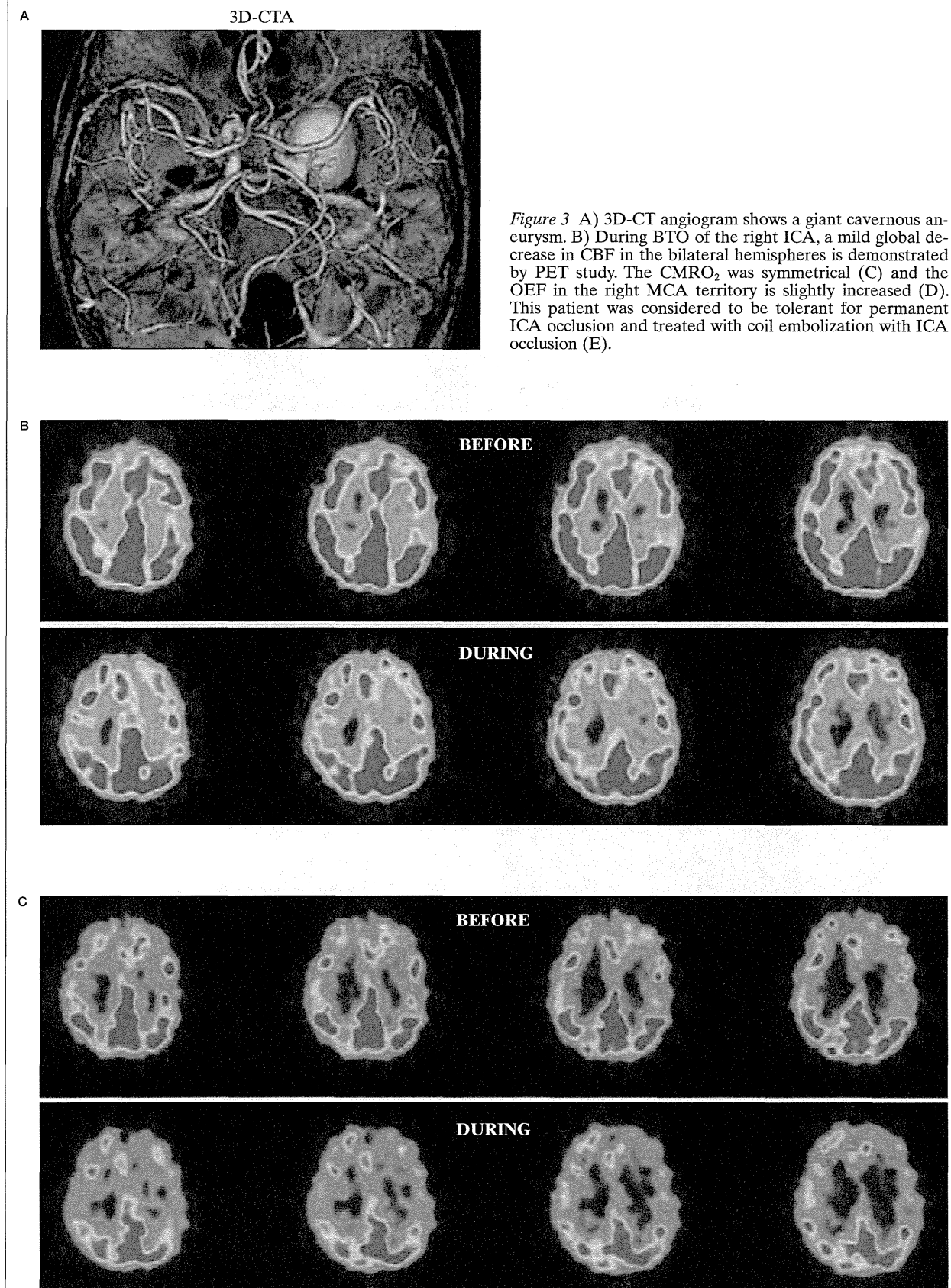

Figure 3 A) 3D-CT angiogram shows a giant cavernous aneurysm. B) During BTO of the right ICA, a mild global decrease in CBF in the bilateral hemispheres is demonstrated by PET study. The $CMRO_2$ was symmetrical (C) and the OEF in the right MCA territory is slightly increased (D). This patient was considered to be tolerant for permanent ICA occlusion and treated with coil embolization with ICA occlusion (E).

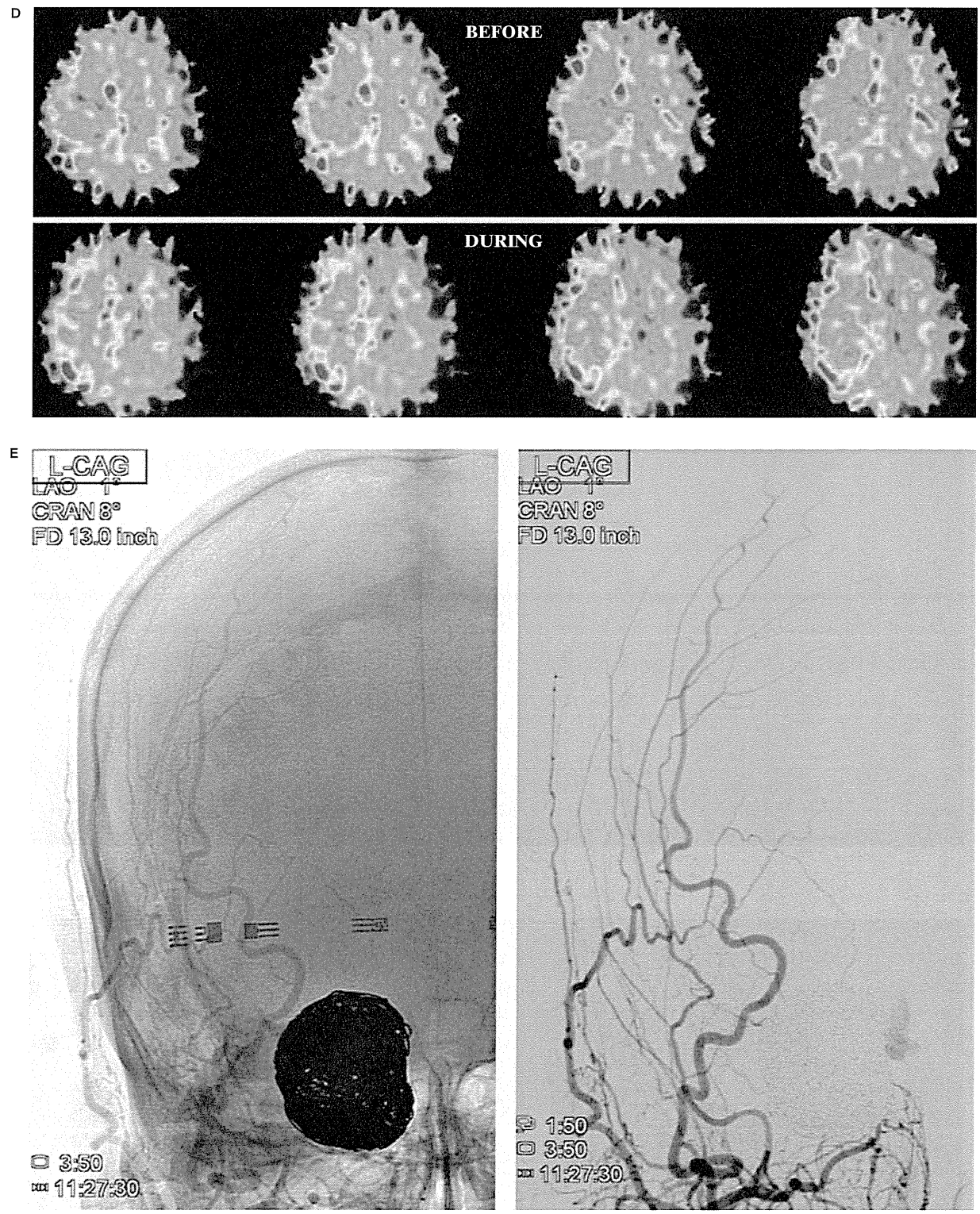

rhage [13]. These values can be quantitatively obtained by PET using ^{15}O-labelled compounds. The computational formulae to compute these parametric images are based on a single-tissue compartment model for oxygen kinetics and generally require a data set of $C^{15}O$ scan for cerebral blood volume (CBV), $C^{15}O_2$ (or $H_2{}^{15}O$) scan for CBF and $^{15}O_2$ scan together with CBF

and CBV values for OEF/$CMRO_2$. Several quantitative approaches have been developed and applied in clinical assessment. In the steady-state method, the parametric images are estimated from the data set that is acquired while in the steady state reached during the continuous inhalation of $^{15}O_2$ and $C^{15}O_2$ as well as bolus inhalation of $C^{15}O$, requiring waiting time to reach equilibrium. This method can be employed using a simple procedure and mathematical formula, but requires a prolonged data-acquisition time (approximately 50-60 min). Recently, one of our colleagues developed a dual tracer autoradiographic (DRAG) method to shorten the PET examination period [16]. This method applies sequential administration of dual tracers of $^{15}O_2$ and $C^{15}O_2$ during a single PET scan and computes CBF and $CMRO_2$ autoradiographically. Clinical studies demonstrate the possibility of neglecting or fixing the CBV value in the computation of the OEF and $CMRO_2$ without significant bias in normal controls and patients with cerebrovascular disease [17,26]. In our institution, we introduced the rapid DRAG method two years ago. This change reduced the burden of patients and clinicians and shortened PET examination time from 50 minutes to 15 minutes and enabled us to measure the CBF and OEF/$CMRO_2$ values before and during BTO in succession. To the best of our knowledge, only a few studies have applied the PET evaluation for BTO. Brunberg et al. [5] applied $H_2^{15}O$ PET for quantitative measurement of regional CBF during BTO to predict the adequacy of collateral flow after permanent carotid occlusion. They demonstrated that patients having a CBF reduction to 25-35 ml/100 g/min during balloon occlusion may bear a risk of cerebral infarction after permanent ICA occlusion even when there was no clinical symptom [5]. This is the first report to measure the blood flow and metabolism in the brain using PET before and during BTO. Although we have not clarified critical values of the OEF/$CMRO_2$ during BTO, which may carry the risk of ischemic complications after permanent ICA occlusion, this approach can improve the sensitivity to predict ischemic complication after permanent ICA occlusion. This study is preliminary and should be performed in a greater number of patients. Our study has several limitations and drawbacks. It should be mentioned that while the findings are suggestive they are still preliminary because of the limited number of cases and this represents a possible limitation to the conclusion drawn. Even though PET study can provide more useful information for the patients, movement to radioisotope suite and longer indwelling time of balloon including inflation and deflation in PET room may require further risk-taking. Moreover, compared to intravenous injection of radioisotope, inhalation of gas tracer used in this study requires additional devices and may limit availability in other institutions.

Conclusion

Measurement of the CBF and OEF/CMRO2 using a new, rapid PET protocol before and during BTO is feasible. With its quantitative character and brief scanning time, our rapid PET can offer a suitable method for predicting tolerance to ICA occlusion. This method may further improve the precision of the test and to reduce the risk of complications following ICA sacrifice with surgery.

Acknowledgment

This study was supported by a Grant-in-Aid for Scientific Research (C) (21591845) from the Ministry of Education, Science and Culture of Japan.

References

1 Maves MD, Bruns MD, Keenan MJ. Carotid artery resection for head neck cancer. Ann Otol Rhinol Laryngol. 1992; 10: 778-781.
2 Shimizu H, Matsumoto Y, Tominaga T. Parent artery occlusion with bypass surgery for the treatment of internal carotid artery aneurysms: clinical and hemodynamic results. Clin Neurol Neurosurg. 2010; 112: 32-39.
3 Linskey ME, Jungreis CA, Yonas H, et al. Stroke risk after abrupt internal carotid artery sacrifice: accuracy of preoperative assessment with balloon test occlusion and stable xenon- enhanced CT. Am J Neuroradiol. 1994; 15: 829-843.
4 Tomura N, Omachi K, Takahashi S, et al. Comparison of technetium Tc 99m hexamethylpropyleneamine oxime single- photon emission tomography with stump pressure during balloon occlusion test of the internal carotid artery. Am J Neuroradiol. 2005; 26: 1937-1942.
5 Brunberg JA, Frey KA, Horton JA, et al. [^{15}O]H_2O positron emission tomography determination of cerebral blood flow during balloon test occlusion of the internal carotid artery. AJNR Am J Neuroradiol. 1994; 15: 725-732.
6 Field M, Jungreis CA, Chengelis N, et al. Symptomatic cavernous sinus aneurysms: management and outcome after carotid artery occlusion and selective cerebral revascularization. Am J Neuroradiol. 2003; 24: 1200-1207.
7 Katano H, Nagai H, Mase M, et al. Measurement of regional cerebral blood flow with $H_2{}^{15}O$ positron emission tomography during Matas Test. Acta Neurochir (Wien). 1995; 135: 70-77.
8 Kato K, Tomura N, Takahashi S, et al. Balloon occlusion test of the internal carotid artery: correlation with stump pressure and ^{99m}Tc- HMPAO SPECT. Acta Radiol. 2006; 47: 1073-1078.
9 Marshall RS, Lazar RM, Young WL, et al. Clinical utility of quantitative cerebral blood flow measurements during internal carotid artery test occlusion. Neurosurgery. 2002; 50: 996-1005.
10 Murphy KJ, Deveikisz JP, Brunberg JA, et al. [O-15] H_2O positron emission tomography determination of cerebral blood flow reserve after intravenous acetazolamide during balloon test occlusion of the internal carotid artery. Interv Neuroradiol. 1998; 30: 57-62.
11 Larson JJ, Tew JM Jr, Tomsick TA, et al. Treatment of aneurysms of the internal carotid artery by intravascular balloon occlusion: long-term follow-up of 58 patients. Neurosurgery. 1995; 36: 26-30.
12 Lorberboym M, Pandit N, Machac J, et al. Brain perfusion imaging during preoperative temporary balloon occlusion of the internal carotid artery. J Nucl Med. 1996; 37: 415-419.
13 Carpenter DA, Grubb RL Jr, Temple LW, et al. Cerebral oxygen metabolism after aneurysmal subarachnoid hemorrhage. J Cereb Blood Flow Metab. 1991; 11: 837-844.
14 Frykholm P, Andersson JLR, Valtysson J, et al. A metabolic threshold of irreversible ischemia demonstrated by PET in a middle cerebral artery occlusion- reperfusion primate model. Acta Neurol Scand. 2000; 102: 18-26.
15 Frykholm P, Hillered L, Långström B, et al. Relationship between cerebral blood flow and oxygen metabolism, and extracellular glucose and lactate concentrations during middle cerebral artery occlusion and reperfusion: a microdialysis and positron emission tomography study in nonhuman primates. J Neurosurg. 2005; 102: 1076-1084.
16 Kudomi N, Hayashi T, Teramoto N, et al. Rapid quantitative measurement of CMRO(2) and CBF by dual administration of (15)O-labeled oxygen and water during a single PET scan-a validation study and error analysis in anesthetized monkeys. J Cereb Blood Flow Metab. 2005; 25: 1209-1224.
17 Kudomi N, Watabe H, Hayashi T, et al. Separation of input function for rapid measurement of quantitative $CMRO_2$ and CBF in a single PET scan with a dual tracer administration method. Phys Med Biol. 2007; 52: 1893-1908.
18 Morishima H, Kurata A, Miyasaka Y, et al. Efficacy of the stump pressure ratio as a guide to the safety of permanent occlusion of the internal carotid artery. Neurol Res. 1998; 20: 732-736.
19 Mathews D, Walker BS, Purdy PD, et al. Brain blood flow SPECT in temporary balloon occlusion of carotid and intracerebral arteries. J Nucl Med. 1993; 34: 1239-1243.
20 Simonson TM, Ryals TJ, Yuh WT, et al. MR imaging and HMPAO scintigraphy in conjunction with balloon test occlusion: value in predicting sequelae after permanent carotid occlusion. Am J Roentgenol. 1992; 159: 1063-1068.
21 Monsein LH, Jeffery PJ, van Heerden BB, et al. Assessing adequacy of collateral circulation during balloon test occlusion of the internal carotid artery with ^{99m}Tc-HMPAO SPECT. Am J Neuroradiol. 1991; 12: 1045-1051.
22 Palestro CJ, Sen C, Muzinic M, et al. Assessing collateral cerebral perfusion with technetium-99m-HMPAO SPECT during temporary internal carotid artery occlusion. J Nucl Med. 1993; 34: 1235-1238.
23 Tanaka F, Nishizawa S, Yonekura Y, et al. Changes in cerebral blood flow induced by balloon test occlusion of the internal carotid artery under hypotension. Eur J Nucl Med.1995; 22: 1268-1273.
24 Yonas H, Linskey M, Johnson DW, et al. Internal carotid balloon test occlusion does require quantitative CBF. Am J Neuroradiol. 1992; 12: 1147-1152.
25 Witt JP, Yonas H, Jungreis C. Cerebral blood flow response pattern during balloon test occlusion of the internal carotid artery. Am J Neuroradiol. 1994; 15: 847-856.
26 Sasakawa Y, Kudomi N, Yamamoto Y, et al. Omission of [15O]CO scan for PET $CMRO_2$ examination using ^{15}O-labelled compounds. Ann Nucl Med. 2011; 25: 189-196.

Nobuyuki Kawai, MD
Department of Neurological Surgery
Faculty of Medicine, Kagawa University
1750-1 Ikenobe, Miki-cho
Kita-gun, Kagawa 761-0793, Japan
Tel.: +81-87-891-2207
Fax: +81-87-891-2208
E-mail: nobu@med.kagawa-u.ac.jp

Journal of Cerebral Blood Flow & Metabolism (2013) 33, 774–779

www.jcbfm.com

ORIGINAL ARTICLE

Long-term adaptation of cerebral hemodynamic response to somatosensory stimulation during chronic hypoxia in awake mice

Hiroyuki Takuwa[1], Kazuto Masamoto[1,2], Kyoko Yamazaki[1,3], Hiroshi Kawaguchi[1], Yoko Ikoma[1], Yousuke Tajima[1,4], Takayuki Obata[1], Yutaka Tomita[5], Norihiro Suzuki[5], Iwao Kanno[1] and Hiroshi Ito[1]

Effects of chronic hypoxia on hemodynamic response to sensory stimulation were investigated. Using laser-Doppler flowmetry, change in cerebral blood flow (CBF) was measured in awake mice, which were housed in a hypoxic chamber (8% O_2) for 1 month. The degree of increase in CBF evoked by sensory stimulation was gradually decreased over 1 month of chronic hypoxia. No significant reduction of increase in CBF induced by hypercapnia was observed during 1 month. Voltage-sensitive dye (VSD) imaging of the somatosensory cortex showed no significant decrease in neural activation over 1 month, indicating that the reduction of increase in CBF to sensory stimulation was not caused by cerebrovascular or neural dysfunction. The simulation study showed that, when effective diffusivity for oxygen in the capillary bed (D) value increases by chronic hypoxia due to an increase in capillary blood volume, an increase in the cerebral metabolic rate of oxygen utilization during neural activation can occur without any increase in CBF. Although previous study showed no direct effects of acute hypoxia on CBF response, our finding showed that hemodynamic response to neural activation could be modified in response to a change in their balance to energy demand using chronic hypoxia experiments.

Journal of Cerebral Blood Flow & Metabolism (2013) **33,** 774–779; doi:10.1038/jcbfm.2013.16; published online 13 February 2013

Keywords: cerebral blood flow; energy metabolism; hemodynamics; microcirculation; neurovascular unit

INTRODUCTION

The oxygen supply to the brain plays an important role in energy metabolism in tissues, and long-term low oxygen environments cause several adaptation mechanisms.[1,2] In human studies, hypobaric hypoxia at high altitudes has been shown to cause cerebral vasodilatation[3] and increase the cerebral blood flow (*CBF*), blood pressure, and hematocrit.[2,4] In rodent, several long-term adaptations in systemic and cerebral hemodynamics to chronic hypoxia have been observed. Baseline *CBF* increased during the first several days during hypoxia (10% O_2 concentration), and then began to decrease, finally returning to the prehypoxia baseline level after 3 weeks.[2,5] In addition, increases in hematocrit and respiratory rate were observed during 3 weeks of chronic hypoxia. Capillary density in the brain significantly increased,[5,6] and cerebral vasodilatation occurred[7] after several days of chronic hypoxia. These effects on the cerebral vasculature were thought to be associated with hypoxia-inducible factor-1 and angiopoietin-2, whose gene expression levels were activated after several days of hypoxia.[1,8,9]

Although effects of chronic hypoxia on baseline *CBF* and capillary density have been investigated, effects of the hemodynamic response under chronic hypoxia remain unclear. The hemodynamic response to neuronal activation under acute hypoxia was investigated in several studies,[10–13] but it is clear that the animal condition in acute hypoxic experiments is quite different from that in chronic hypoxic experiments. Especially, increases in capillary density, baseline *CBF*, and the diameter of cerebral vessels occur during chronic hypoxia, and such adaptations might affect the hemodynamic responses to neuronal activation. To clarify the long-term changes of *CBF* response to evoked neural activity in the mouse exposed to chronic hypoxia, we measured the cerebrovascular responses to neural activation and hypercapnia in awake mice under chronic hypoxia. The hemodynamic responses were evaluated by laser-Doppler flowmetry (LDF) experiment repeatedly over 1 month of chronic hypoxia in the same mouse somatosensory cortex. Voltage-sensitive dye (VSD) imaging was also performed to assess the effects of chronic hypoxia on neuronal activity. Furthermore, a simulation study was performed to demonstrate the relation between *CBF* and the cerebral metabolic rate of oxygen utilization ($CMRO_2$) during neural activation under the condition of chronic hypoxia.

MATERIALS AND METHODS

Animal Preparation

All experiments were performed in accordance with the institutional guidelines on the humane care and use of laboratory animals and were approved by the Institutional Committee for Animal Experimentation. A total of 24 male C57BL/6J mice (20 to 30 g, 7 to 11 weeks; Japan SLC, Hamamatsu, Japan) were housed in hypoxic chambers at 8% to 9% O_2 concentration and used in two experiments as follows. In the first experiment (experiment I; Figure 1A), LDF measurement during whisker stimulation was performed before ($N=12$) and at 7 days ($N=7$), 14 days ($N=7$) during, and 1 month ($N=7$) after chronic hypoxia. In five animals selected from these animals, LDF measurements during CO_2 inhalation and VSD imaging during whisker stimulation were performed before and

[1]Biophysics Program, Molecular Imaging Center, National Institute of Radiological Sciences, Chiba, Japan; [2]Center for Frontier Science and Engineering, University of Electro-Communications, Tokyo, Japan; [3]Department of Biomedical Engineering, Tokyo University, Tokyo, Japan; [4]Department of Neurological Surgery, Chiba University Graduate School of Medicine, Chiba, Japan and [5]Department of Neurology, Keio University School of medicine, Tokyo, Japan. Correspondence: Dr H Ito, Biophysics Program, Molecular Imaging Center, National Institute of Radiological Sciences, 4-9-1 Anagawa, Inage-ku, Chiba 263-8555, Japan.
E-mail: hito@nirs.go.jp
Received 15 November 2012; revised 11 January 2013; accepted 25 January 2013; published online 13 February 2013

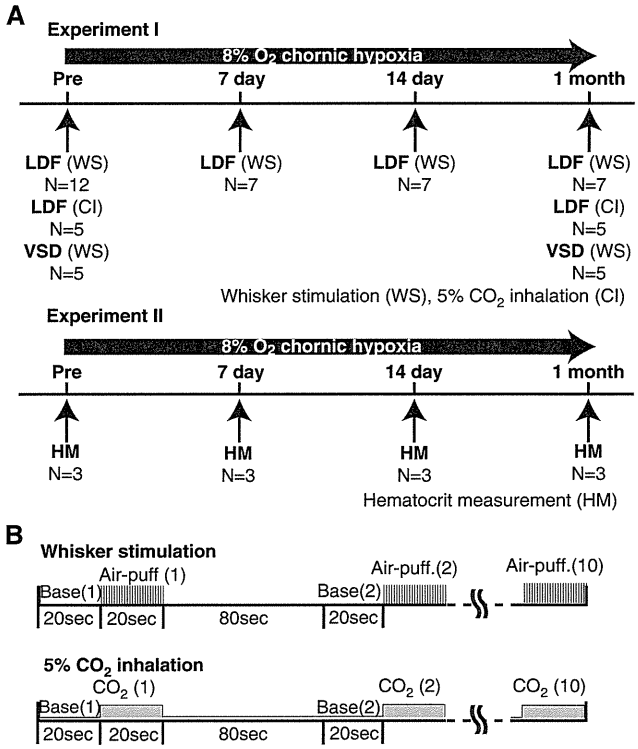

Figure 1. (**A**) Experiment I (laser-Doppler flowmetry (LDF) measurement and voltage-sensitive dye (VSD) imaging in awake animals) and experiment II (hematocrit measurement). LDF measurement during whisker stimulation was performed before ($N = 12$) and 7 days ($N = 7$), 14 days ($N = 7$), and 1 month ($N = 7$) after the start of chronic hypoxia. In five of these animals, LDF measurements during CO_2 inhalation and VSD imaging during whisker stimulation were performed before and 1 month after chronic hypoxia. In experiment II, hematocrit measurement was performed in a total of 12 animals (each measurement used three animals) before, at 7 days and 14 days during, and 1 month after chronic hypoxia. Hematocrit was estimated with a blood analyzer (I-STAT; Abbott). (**B**) Experimental protocols of whisker stimulation and 5% CO_2 inhalation. In whisker stimulation, 20 seconds of rectangular pulse air-puff stimulation (50-milliseconds pulse width and 100-milliseconds onset-to-onset interval, i.e., 10 Hz frequency) was given to the right whisker region of mice. Ten consecutive trials were repeated with an onset-to-onset interval of 120 seconds in each experiment. In CO_2 inhalation, 5% CO_2 gas was given to mice continuously for the same duration (20 seconds) and interval (120 seconds) as the sensory stimulation.

1 month after chronic hypoxia. In the second experiment (experiment II; Figure 1A), hematocrit measurement was performed in a total of 12 animals (each measurement used three animals) before, at 7 days, 14 days during, and 1 month after chronic hypoxia. Anesthesia was only used in this experiment II for pain avoidance.

A surgical procedure was applied to prepare a chronic cranial window and fixation to the heads of mice for reproducible stereotaxic measurement for up to 1 month. The animals were anesthetized with a mixture of air, oxygen, and isoflurane (3% to 5% for induction and 2% for surgery) via a facemask. The animals were fixed in a stereotactic frame, and rectal temperature was maintained at 38°C using a heating pad (ATC-210, Unique Medical, Tokyo, Japan). The methods for preparing the chronic cranial window have been reported in detail by Tomita *et al.*[14] A midline incision (10 mm) was made to expose the skull. Craniotomy was performed over the left somatosensory cortex, keeping the dura intact (3 to 4 mm diameter, centered at 1.8 mm caudal, and 2.5 mm lateral from bregma). The brain surface was sealed with a quartz coverslip using dental cement (Ionosit, DMG, Hamburg, Germany) to make the preparation waterproof. A custom metal plate was affixed to the skull with a 7-mm diameter hole centered over the cranial window. After completion of the surgery, the animals were allowed to recover from anesthesia and housed for at least 7 days before initiation of the experiments.

Exposure to Chronic Hypoxia

From 1 week after the cranial window surgery, the mice were kept for up to 1 month in hypoxic chambers (8% to 9% O_2 in N_2) with food and water provided *ad libitum*. The chamber was a fully sealed plastic box (200 mm long, 150 mm wide, and 100 mm high) with two nozzles. One nozzle, attached to the lateral side of the chamber, was connected to a gas blender (GB-2C, KOFLOC, Kyoto, Japan) to deliver the hypoxic gas mixture into the chamber. The second nozzle was used to flush out the gas mixture. The hypoxic gas was regulated by gas blender, and the O_2 levels in the chamber were monitored every day using an oxygen sensor (OPA-5000E, KITAGAWA, Kanazawa, Japan). During chronic hypoxia, the mean oxygen concentration in the chamber was 8.6% ± 0.2%, indicating that the hypoxic chamber was maintained within our target range (8% to 9% O_2). The temperature in the chamber was controlled at ~23°C (range 22°C to 24°C) with a room air conditioner. Two animals per chamber were housed in each experiment for a maximum of up to 1 month. The chamber was opened for 10 minutes every 3 days for cleaning and animal care.

Laser-Doppler Flowmetry Measurement

The animals were moved from a hypoxic chamber to a recording room, and the measurement was conducted under normoxic condition. The body weight of the animal was measured, and then the head was fixed to a custom-made stereotactic apparatus with a floating ball device that allowed the animal to move freely during the recording of LDF.[15] Evoked *CBF* was measured with laser-Doppler flowmetry (FLO-C1, OMEGAWAVE, Tokyo, Japan), as described previously.[16] The tip of the LDF probe (Type NS, OMEGAWAVE) was positioned over the whisker stimulation-induced activated cortex on the cranial window while avoiding large blood vessel areas. The activated hot spot was preliminarily determined by screening the response to sensory stimulation at several points in the somatosensory area. Then, the *X–Y* position of the LDF tip was marked on the edge of the cranial window for reproducible placement of the LDF tip. The angle of the LDF probe to the cortex was fixed by manipulator, perpendicular to the cranial window surface. Also, the distance between the LDF tip and the surface of the cranial window was maintained among the different experiments. On each day of the experiments, the level constancy of the reflected light signal for the LDF measurements was confirmed before initiation of the recording.

The time course of the LDF signal changes was recorded using a polygraph data acquisition system (MP150, BIOPAC Systems, Goleta, CA, USA) at a sampling rate of 200 Hz and analyzed offline. For each trial of the experiment, the LDF signal was normalized by the 20-second prestimulus baseline level, and averaged across 10 trials. For the whisker stimulation experiments, the magnitude of evoked *CBF* was calculated as the mean percentage change for 20-seconds stimulation periods relative to baseline. In the case of CO_2 inhalation, the mean percentage increase in *CBF* was calculated from 10 to 20 seconds of the stimulation period, because the increase in *CBF* usually started 5 to 10 seconds after inhalation. Statistical analysis was performed to compare the evoked *CBF* across different experimental days using one-way analysis of variance followed by Tukey's test.

Voltage-Sensitive Dye Imaging

The cerebral cortex was stained with RH1691 (Optical Imaging, Rehovot, Israel) via transdura delivery for 2 hours and rinsed with dye-free saline for 30 seconds. Dye and saline were injected through a metal tube (500-μm inside-diameter), which was connected to a space between the cranial window and dura through one side of the cranial window. Then, the mice were fixed onto the apparatus while keeping an awake-state. The excitation light was 632 ± 10 nm, and a fluorescent light from the stained cortex was passed through a dichroic mirror and long-pass filter (>660 nm).[15] The image was obtained using a 128-channel photodiode array at a rate of 1 kHz. The *X–Y* in-plane resolution was 250 × 250 μm^2.

For the analysis of VSDI signals, independent component analysis was applied to exclude systemic physiological noise originating from the heartbeat and respiration.[15] Then, all of the VSDI signals were normalized to the maximal response measured over 128 channels. The whisker stimulation-induced activated region was determined by measuring the number of pixels at which the normalized VSD signal was greater than an intensity threshold of 0.5 (maximum pixel intensity 1.0). Comparison of the activated region was made between pre- and posthypoxia conditions, and statistical analysis was performed by paired *t*-test.

Whisker Stimulation

Compressed air (up to 10 psi) was generated with an air compressor (NUP-2, AS ONE, Osaka, Japan), and the pressure was controlled with a Pico Pump (PV830, WPI, Osaka, Japan). The compressed air pulse was delivered to the entire right whisker region from a nozzle placed ~1 cm away from the mouse.[16] Twenty seconds rectangular pulse stimulation (50-milliseconds pulse width and 100-milliseconds onset-to-onset interval, i.e., 10 Hz frequency) was generated with Master-8 (A.M.P.I, Jerusalem, Israel). In each experiment, 10 consecutive trials were repeated with an onset-to-onset interval of 120 seconds (Figure 1B).

Hypercapnia (5% CO_2 Inhalation)

A hypercapnic gas mixture of 5% CO_2, 21% O_2, and residual N_2 was inhaled by awake-behaving mice via a facemask (300 mL/min). At all times except during the CO_2 inhalation, the mice inhaled room air (300 mL/min). CO_2 gas was given to the mice for the same duration (20 seconds) and interval (120 seconds) as the sensory stimulation using the Master 8 (Figure 1B). CO_2 inhalation was repeated 10 times, and the LDF signals were averaged offline.

Experiment II: Hematocrit Measurement

Hematocrit measurement was performed in total 12 animals (each measurement used three animals) before, at 7 days, 14 days, and 1 month after the start of chronic hypoxia. Because mice under hematocrit measurement, which severely influenced the physiological state, were unsuitable for the long-term LDF and VSDI experiment, those in experiment II were different from those in experiment I. In the experiment, the mice were moved from the hypoxic chambers and exposed to room air. They were anesthetized with isoflurane (3% to 5% for induction and 2% for surgery) using facemasks. Body temperature was monitored with a rectal probe and maintained at ~37.0°C with a heating pad. Heart blood samples were obtained with a needle (23 gauge) before and after 7 days, 14 days, and 30 days of hypoxic chamber exposure (Figure 1A). The hematocrit level was analyzed with a blood analyzer (I-STAT; Abbott, Chicago, IL, USA).

Simulation Study

To evaluate the relation between *CBF* and $CMRO_2$ during neural activation under the condition of chronic hypoxia, a simulation study was performed. The effective diffusivity for oxygen in the capillary bed (*D*) was defined as $OEF = 1 - e^{(-D/CBF)}$, where *OEF* is the oxygen extraction fraction.[17] Cerebral metabolic rate of oxygen utilization can be calculated as $CMRO_2 = C_a \bullet CBF \bullet OEF$, where C_a is the total oxygen content in arterial blood. Thus, the relation between changes in *CBF* and $CMRO_2$ during neural activation should depend on *D*. Assuming the baseline *CBF* for mouse as 100 mL per 100 mL per minute[17] and baseline *OEF* to be 0.2,[18] *D* can be calculated to be 0.223 mL per mL per minute. The *D* value is proportional to the capillary blood volume,[19] and a 40% to 70% increase in capillary diameter by chronic hypoxia has been reported in mice using two-photon laser microscopy,[7] corresponding to a 96% to 189% increase in capillary blood volume and, therefore, in *D*. Thus, the relation between changes in *CBF* and $CMRO_2$ during neural activation was simulated for *D* values of 0.223 (baseline), 0.245 (10% increase), 0.268 (20% increase), 0.335 (50% increase), 0.446 (100% increase), and 0.669 (200% increase) mL per mL per minute.

RESULTS

Change in Systemic Hematocrit and Body Weight During Chronic Hypoxia

The body weights before and after 7 days, 14 days, and 1 month of exposure to chronic hypoxia were 23.3 ± 2.3 g, 22.2 ± 2.2 g, 20.7 ± 1.6 g, and 22.0 ± 1.4 g, respectively. There was no significant difference in body weight among the respective measurement days. On the other hand, when control mice were housed in a normoxic chamber, body weights significantly increased over one month (day 0: 23.8 ± 2.2 g, day 30: 26.4 ± 2.4 g, $P<0.01$, $N=6$). Therefore, it was possible that chronic hypoxia inhibited the weight gain of mice over the month. Hematocrit was significantly higher ($P<0.01$) at 7 days (51.5%), 14 days (59.0%), and 1 month (68.5%) from the start of exposure to chronic hypoxia as compared with control mice (34.6%). These results were in good agreement with previous studies conducted in rats and mice under chronic hypoxia.[10]

Cerebral Blood Flow Response to Sensory Stimulation

Time–response curves of the increase in *CBF* during whisker stimulation during 1 month of chronic hypoxia are shown in Figure 2. The mean percentage increases were 20.3% ± 6.8%, 13.1% ± 3.3%, 9.9% ± 4.2%, and 3.9% ± 4.0% before and after 7 days, 14 days, and 1 month of chronic hypoxia, respectively (Figure 3). Statistically significant differences were found at day 7 ($P<0.05$), day 14 ($P<0.01$), and 1 month ($P<0.01$) of chronic hypoxia, compared with that of prehypoxic control.

Cerebral Blood Flow Response to 5% CO_2 Inhalation

The time–response curve of the increase in *CBF* during 5% CO_2 inhalation before chronic hypoxia was almost identical to that after 1 month of hypoxia (Figure 4A). The mean percentage increase in *CBF* induced by 5% CO_2 inhalation was 14.8% ± 3.5% and 16.3% ± 4.0% before and 1 month after chronic hypoxia, respectively (Figure 4B). There was no significant difference in the increase in *CBF* between the measurements before and 1 month after chronic hypoxia.

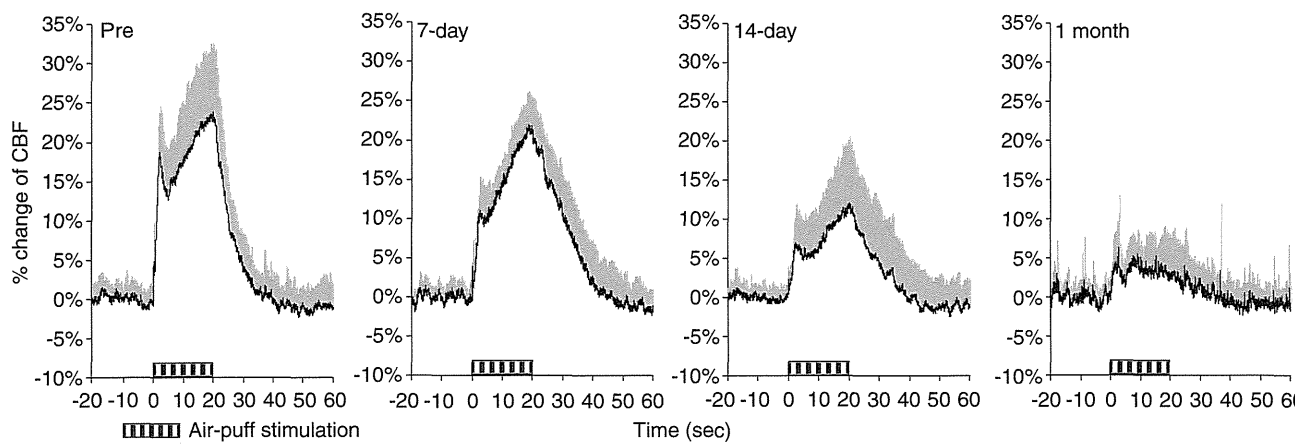

Figure 2. Time–response curves for normalized increase in cerebral blood flow (*CBF*) response to sensory stimulation during chronic hypoxia. Horizontal bars indicate the stimulation period. These data were normalized to baseline level (20 seconds before sensory stimulation). Each response curve represents the mean of all animals at each measurement day. Error bars indicate s.d.